



FUMEX 2

IAEA Coordinated Research Programme

2002-2006



Nuclear Fuel Cycle and Material Section



Purpose

Describe the IAEA fuel modelling project

Show some of the participants' Code Predictions

Discuss PCI modelling

Discuss high burnup problems

Show experimental evidence addressing these issues



FUMEX-II

The International Atomic Energy Agency is sponsoring a Coordinated Research Project on Fuel Modelling at Extended Burnup (FUMEX-II). Nineteen fuel modelling groups are participating with the intention of improving their capabilities to understand and predict the behaviour of water reactor fuel at high burnups. The exercise is carried in coordination with the OECD/NEA.



FUMEX-II

Purpose:

The major objective of the IAEA Coordinated Research Project (CRP) is to improve the predictive capabilities of codes used in fuel behaviour modelling for extended burn-up.

In addition, the CRP address the performance of codes used for transient analysis such as RIA and LOCA at extended burnup.



FUMEX-II

Purpose

The focus is on the topics:

- Thermal performance
 - Fission gas release
 - Pellet to clad interaction (PCI)
- at extended burn-up above 50 MWd/kg.



CRP FUMEX-II

List of Participants

No.	Country	Name of Chief Scientific Investigator	Institute	Title of Project
1	Argentina	Mr. M. Armando	CNEA	Improvement of models used for fuel behaviour
2	Belgium	Mr. V. Sobolov	Nuclear Research Center SCK CEN	Fuel performance modelling at SCK*CEN
3	Bulgaria	Mr. D. Elenkov	Institute for Nuclear Research and Nuclear Energy	Improvement of the TRANSURANUS-WWER version code for modelling WWER-fuel performance
4	Czech Republic	Mr. M. Valach	Nuclear Research Institute, Rez	Validation of fuel performance codes used at the NRI Rez for the Temelin and Dukovany NPPs fuel safety evaluations and operation support
5	China	Mr. P. Chen	China Institute of Atomic Energy	Validation of fuel behavior analysis code METEOR/TR by using the data of FUMEX II exercises
6	EC	Dr P. van Uffelen	JRC Institute for Transuranium Elements	Application of the TRANSURANUS code in the FUMEX II programme
7	Germany France	Mr. F. Sontheimer	FRAMATOME ANP GmbH	Improvement of high burnup models for fuel temperature and FG release in Framatome ANP fuel rod performance codes
8	Korea Republic, of	Mr.Chan Bock Lee	Korea Atomic Energy Research Institute	Improvement and validation of fuel performance analysis code INERA
9	Romania	Ms. A. Paraschiv	Institute for Nuclear Research	New methods of evaluation the nuclear oxide fuel behavior
10	RF	Mr. G. Khvostov	A.A. Bochvar Res. Institute of Inorganic Materials	Improvement and verification of the START-3 code
11	Canada	Mr. M. Tayal	AECL	Simulation of FUMEX II data by ELESTRES Code
12	India	Mr. H.S. Kushwaha	BARC	Validation and Improvement of Indian Codes for Fuel Performance for High Burnup Application
13	UK	Mr. T. Turnbull		Qualification of fuel performance codes and datasets
14	Japan	Mr. K. Kamimura	NUPEC	Validation of the FEMAXI-JINS code by using PIE data at extended burnup
15	Finland	Mr. K. Ranta-Puska	VTT	Validation of the ENIGMA fuel performance code



CRP FUMEX-II

List of Observers

Ms S. Stefanova, INRE Bulgaria:	PIN code
Mr A. Nordstroem, PSI, Switzerland:	PSI version TRANSURANUS
Mr G. Rossiter, BNFL, UK:	ENIGMA-B
Mr K. Atkinson, British Energy, UK:	ENIGMA



FUMEX-II

The participants are using a mixture of data derived from actual irradiation histories of high burnup experimental fuel and commercial irradiations where post-irradiation examination measurements are available, combined with idealised power histories intended to represent possible future extended dwell commercial irradiations and test code capabilities at high burnup.

All participants have been asked to model six priority cases out of some 27 cases made available to them for the exercise from the IAEA/OECD/NEA Irradiated Fuel Performance Experimental Database.



FUMEX - II

List of high priority cases

No.	Case identification	Measurements made for comparison
3.	Halden IFA 597.3, rod 7	Cladding elongation, at Bu \approx 60 MWd/kgUO ₂
4.	Halden IFA 597.3, rod 8	FCT, FGR at Bu \approx 60 MWd/kgUO ₂
7.	REGATE	FGR and cladding diameter during and after a transient at Bu \approx 47 MWd/kg
14.	Riso-3 AN3	FGR and pressure-EOL, FCT, Bu \approx 37 MWd/kgUO ₂
15.	Riso-3 AN4	FGR and pressure-EOL, FCT, Bu \approx 37 MWd/kgUO ₂
27	Simplified case	(1) Temperature vs Bu for onset of FGR
		(2a) FGR for constant 15 kW/m to 100 MWd/kgU
		(2b) FGR for 20 kW/m at BOL decreasing linearly to 10 kW/m at 100 MWd/kgU
		(2c) FGR for idealized history supplied by BNFL
		(2d) FGR for idealized history supplied by FANP
		(3a) FGR for CANDU idealized history
		(3b) FGR for CANDU idealized history



FUMEX-II

Calculations carried out by the participants, particularly for the idealised cases, have shown how varying modelling assumptions affect the high burnup predictions, and have led to an understanding of the requirements of future high burnup experimental data to help discriminate between modelling assumptions. This understanding is important in trying to model transient and fault behaviour at high burnup.



FUMEX-II

It is important to recognise that the code predictions presented here should not be taken to indicate that some codes do not perform well. The codes have been designed for different applications and have differing assumptions and validation ranges; for example codes intended to predict CANDU fuel operation with thin wall collapsible cladding do not need all the complicated clad creep and gap conductivity modelling found in PWR codes. Therefore, when a case is based on CANDU technology or PWR technology, it is to be expected that the codes may not agree.

However, it is the very differences in such behaviour that is useful in helping to understand the effects of such internal modelling.



FUMEX-II

FUMEX-II is a successor to the first IAEA FUMEX exercise and takes the form of co-ordination between a Code Improvement Exercise and the NEA/IAEA International Fuel Performance Experiments (IFPE) Database. The dual advantages of this co-operation are:

- Exposure of code developers to a wide ranging database;
- Assistance in qualification of the IFPE database, correction of errors and detection of missing data, brought about by use of the database for comparison of predictions with data by a large number of workers.



The Irradiated Fuel Performance Experimental Database (IFPE)

The aim of the International Fuel Performance Experimental Database (IFPE Database) is to provide, in the public domain, a comprehensive and well-qualified database on zircaloy-clad UO_2 fuel for model development and code validation.

The data encompass both normal and off-normal operation and include prototypic commercial irradiations as well as experiments performed in Material Testing Reactors. To date, the Database contains over 800 individual cases, providing data on fuel centreline temperatures, dimensional changes and FGR either from in-pile pressure measurements or PIE techniques, including puncturing, Electron Probe Micro Analysis (EPMA) and X-ray Fluorescence (XRF) measurements.



The Irradiated Fuel Performance Experimental Database (IFPE)

This work in assembling and disseminating the Database is carried out in close co-operation and co-ordination between OECD/NEA and the IAEA.

The majority of data sets are dedicated to fuel behaviour under LWR irradiation, and every effort has been made to obtain data representative of BWR, PWR and VVER conditions. In each case, the data set contains information on the pre-characterisation of the fuel, cladding and fuel rod geometry, the irradiation history presented in as much detail as the source documents allow, and finally any in-pile or PIE measurements that were made.

FUMEX-II uses data from the IFPE, and has provided quality assurance and additional data.



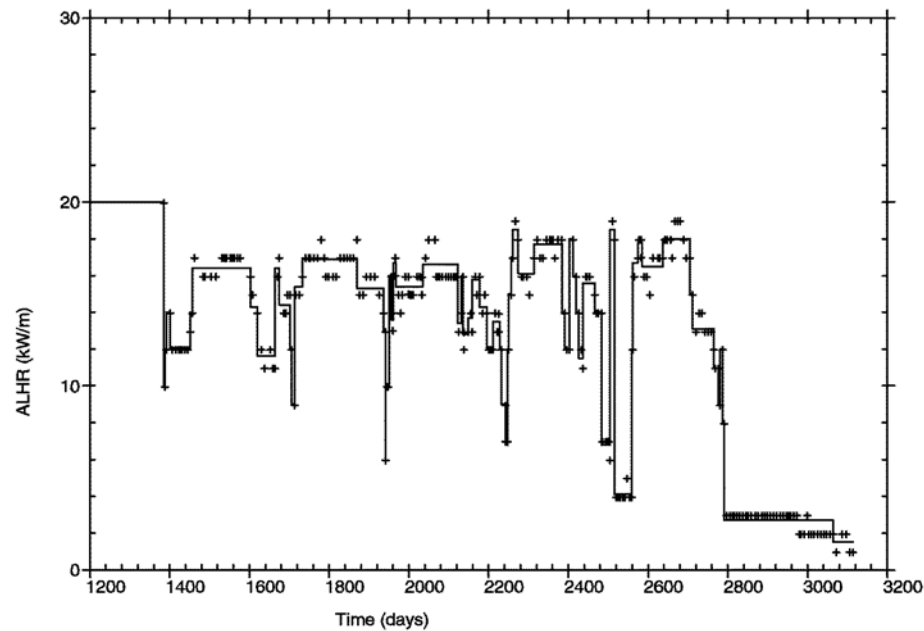
Agreed high priority cases

- IFA-597 rod 8 (high burn-up)
thermocouple temperature versus local power in first ramps
- Riso 3 rod AN3 (helium fill)
thermocouple temperature versus local power in first ramps
- Riso 3 rod AN4 (xenon fill)
thermocouple temperature versus local power in first ramps
- Simplified cases
 - 27(1) Temperature versus Burn-up for FGR onset
 - 27(2a) FGR for constant 15 kW/m to 100MWd/kgU
 - 27(2b) FGR for 20 kW/m at BOL reducing linearly to 15 kW/m at 100 MWd/kgU
 - 27(2c) FGR for BNFL idealized history
 - 27(2d) FGR for FANP idealized history



FUMEX-2 Case 3 IFA-597.2 & .3

Ringhals -1 Base Irradiation History



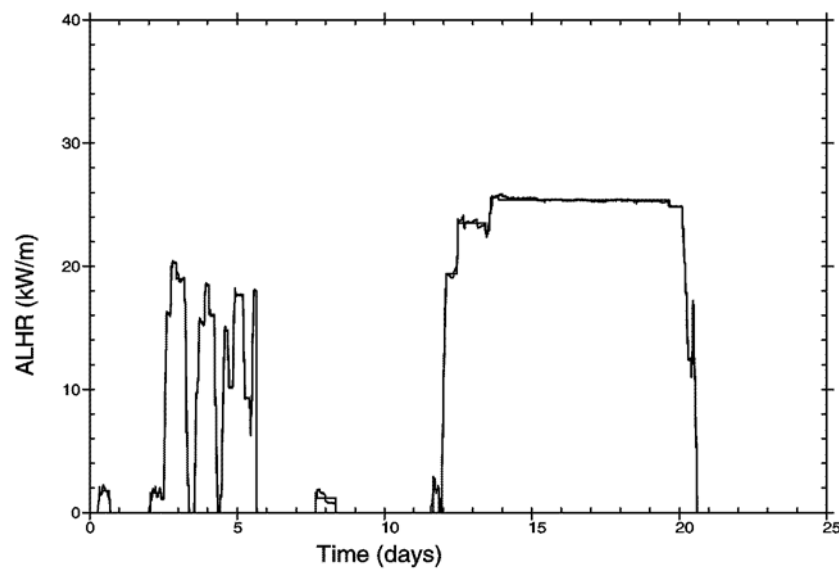
- Flat axial power profile
- 4 axial zones:
top, middle, bottom and TF position
- Low average power
- Long irradiation time
- 59 MWd/kgUO₂
- 2.5-3.3% FGR
- >200 micron HBS at pellet rim



FUMEX-2 Case 3 IFA-597.2 & .3

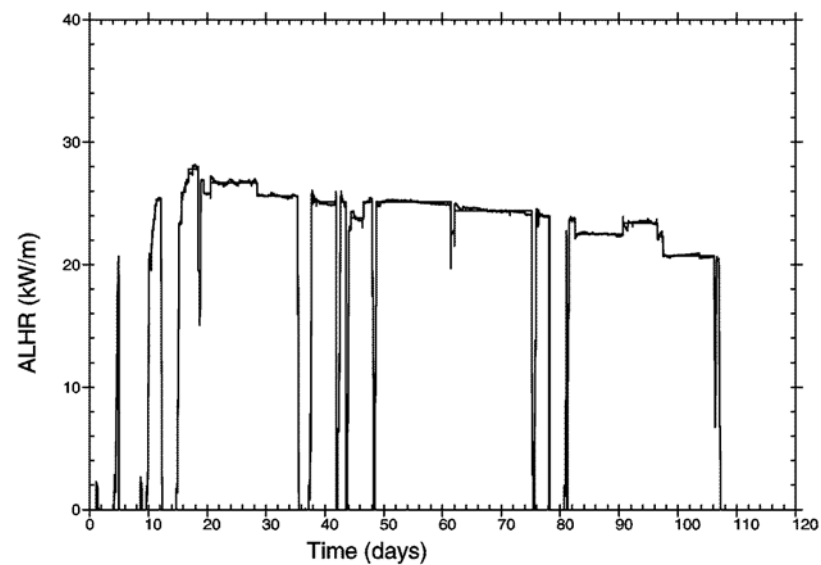
Halden Irradiation Histories

Rod 8, rod 9 similar



Loading 2

Rod 8, rod 7 similar

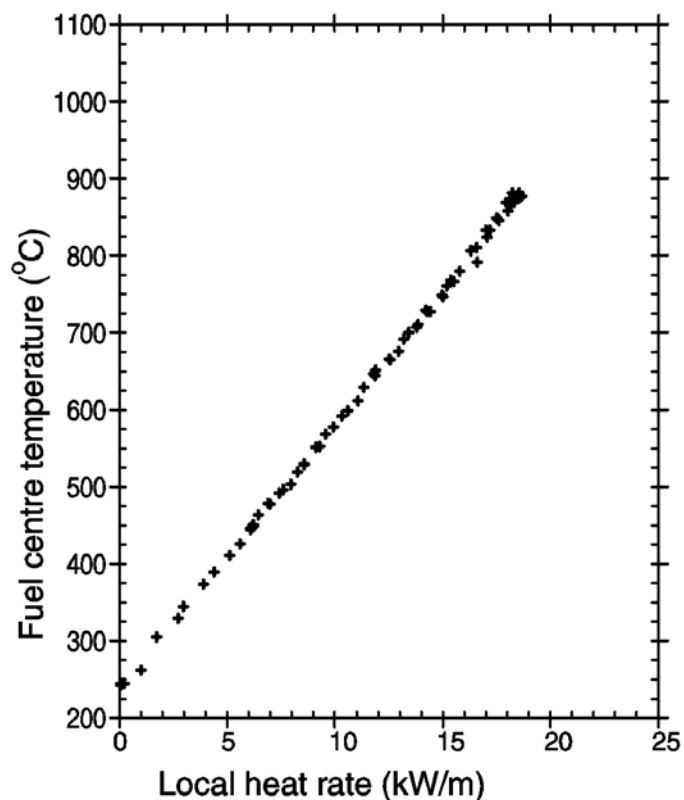


Loading 3



FUMEX-2 Case 4 IFA-597.3

Temperature data for rod 8 during first series of ramps

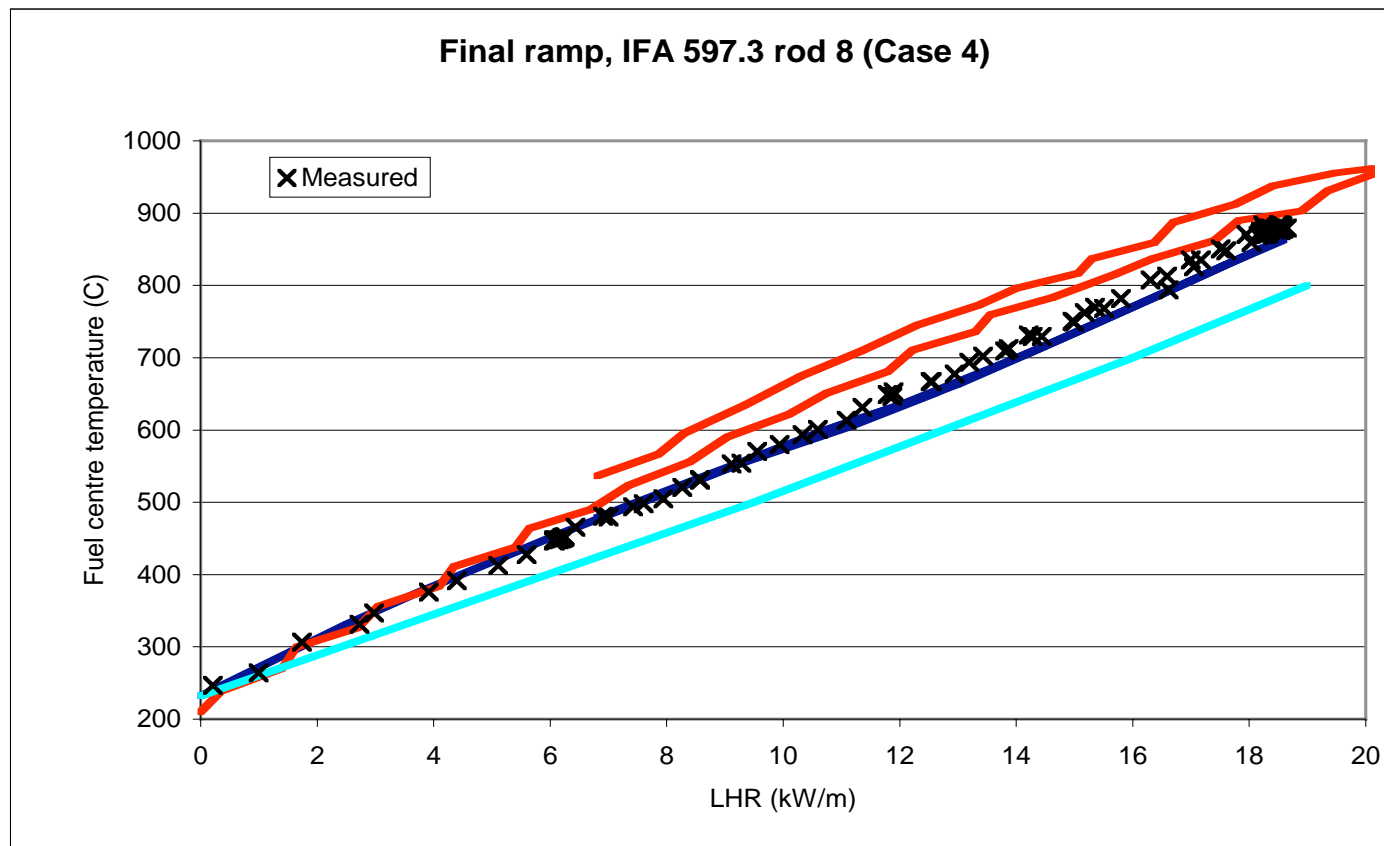


- 59 MWd/kgUO₂
- Closed gap
- No fission gas contamination
- >200 micron HBS at pellet rim
- Data also for rod 9
- Data also for rod 8 at end of irradiation



Temperature Modelling of Ramp Tests

Figure 1: Fuel centre temperature modelling for IFA 597.3 Rod 8. Power ramp at 60MWd/kgUO₂

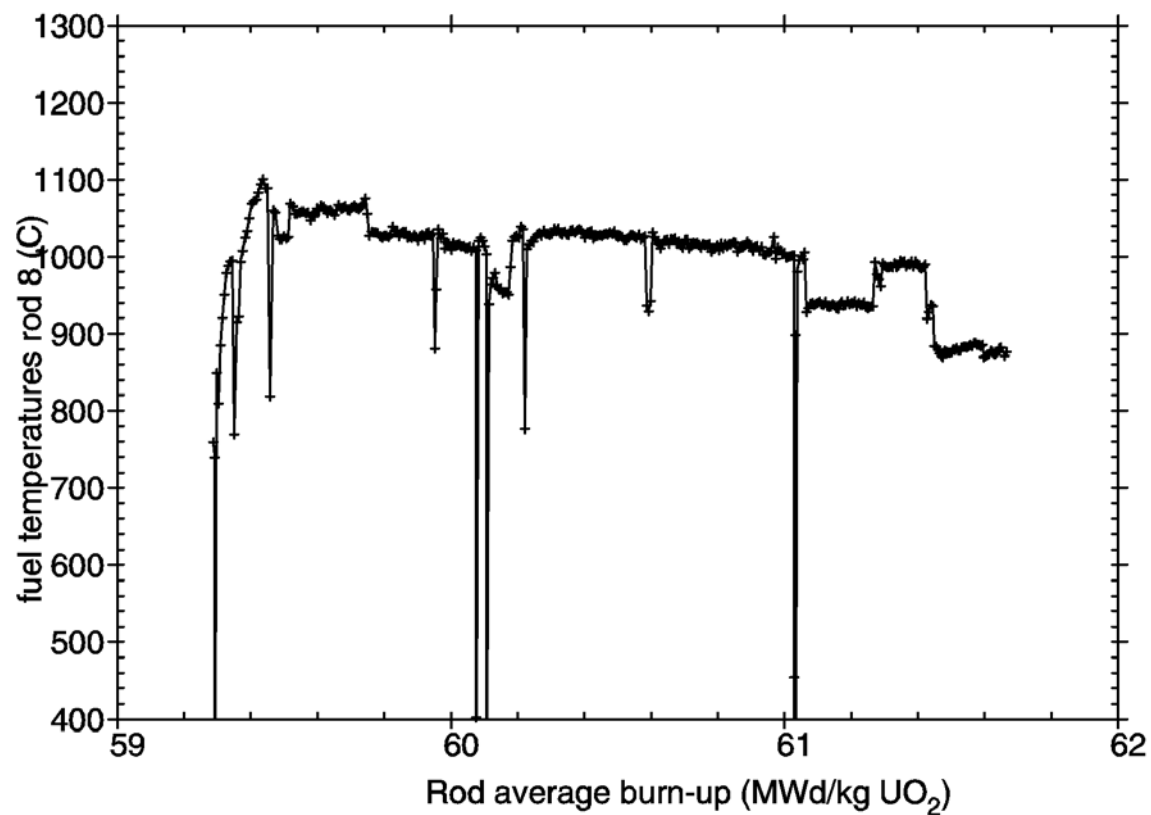


Predictions of three codes against the fuel centre temperature from the final ramp of the Halden experiment IFA 597.3 rod 8 which was carried out when the rod had reached 60MWd/kgUO₂. The predictions shown tend to bound the results from the other modelling teams and it is clear that overall the modelling of fuel centre temperature at this high burnup has been very successful.



FUMEX-2 Case 4 IFA-597.3

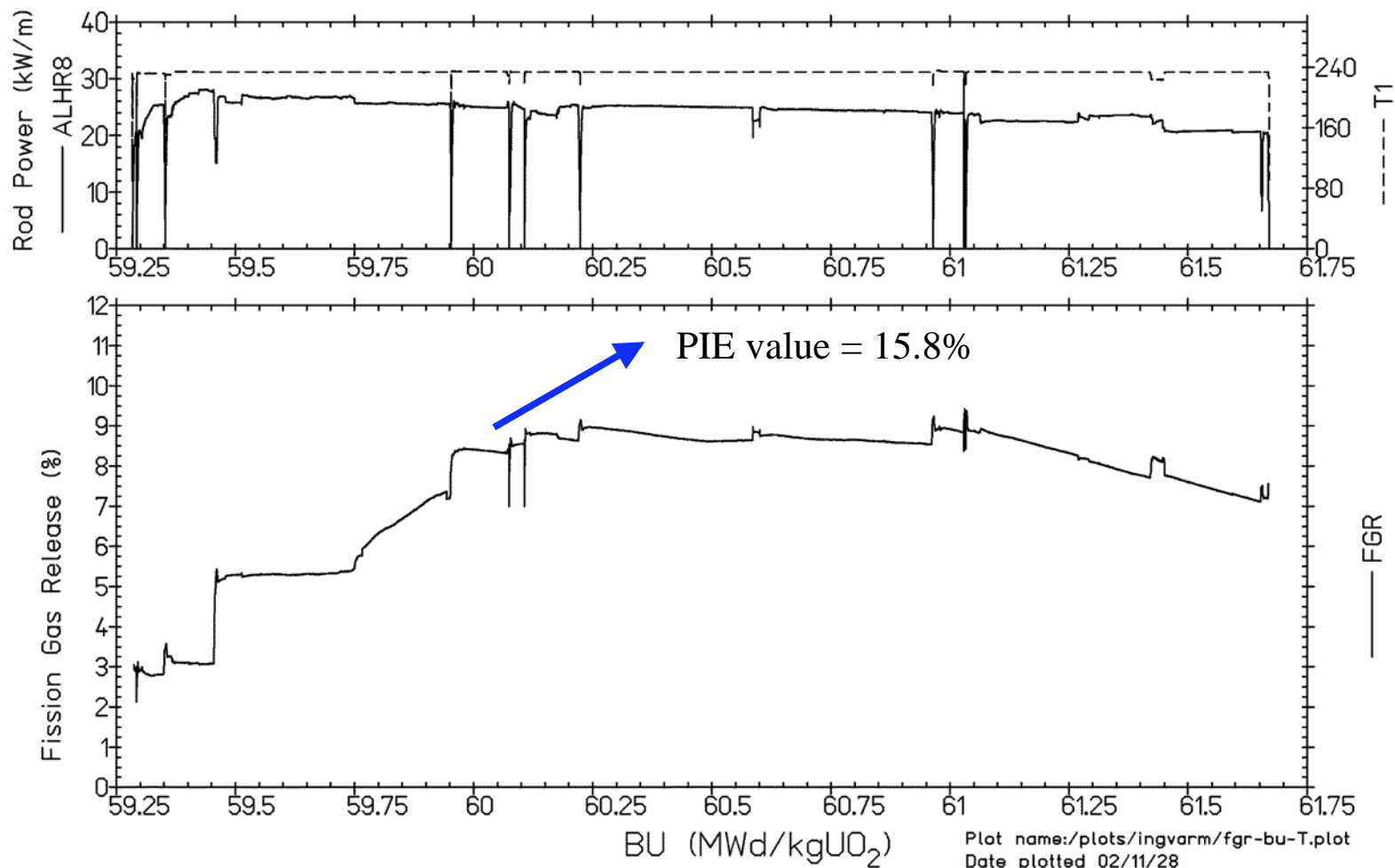
Temperature data for rod 8 during 3rd loading





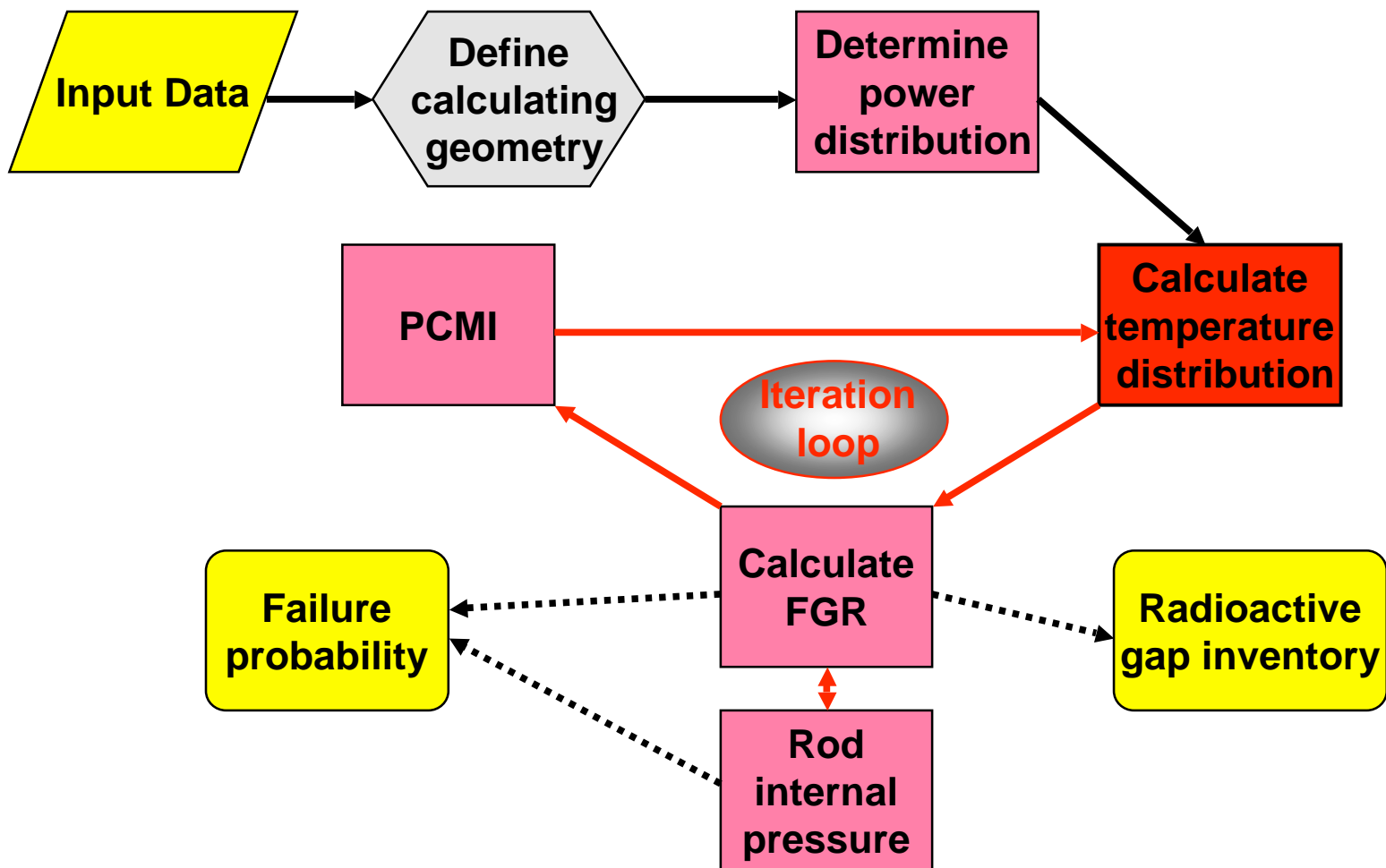
FUMEX-2 Case 4 IFA-597.3

FGR derived from pressure measurements for rod 8 during 3rd loading



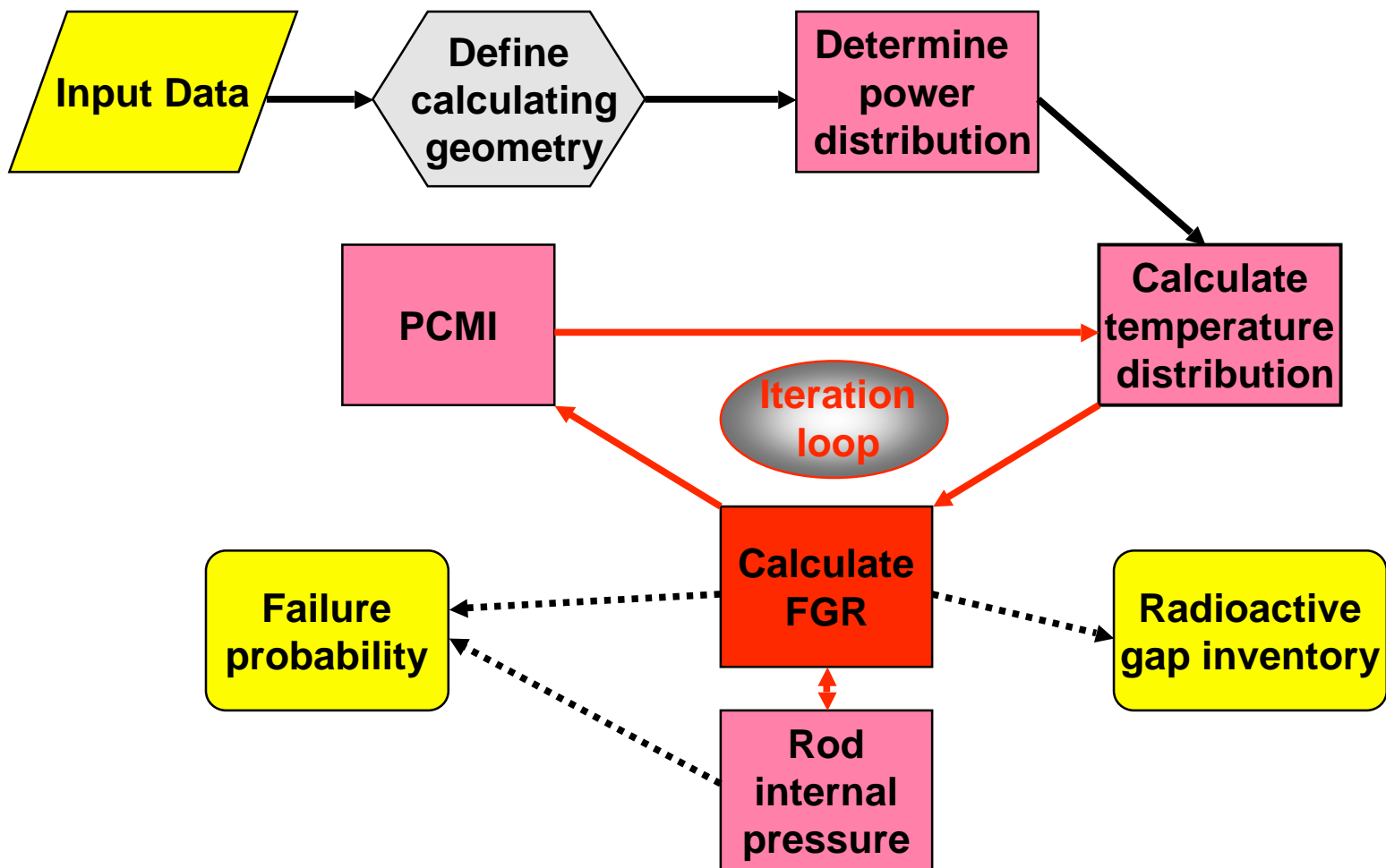


Typical code structure





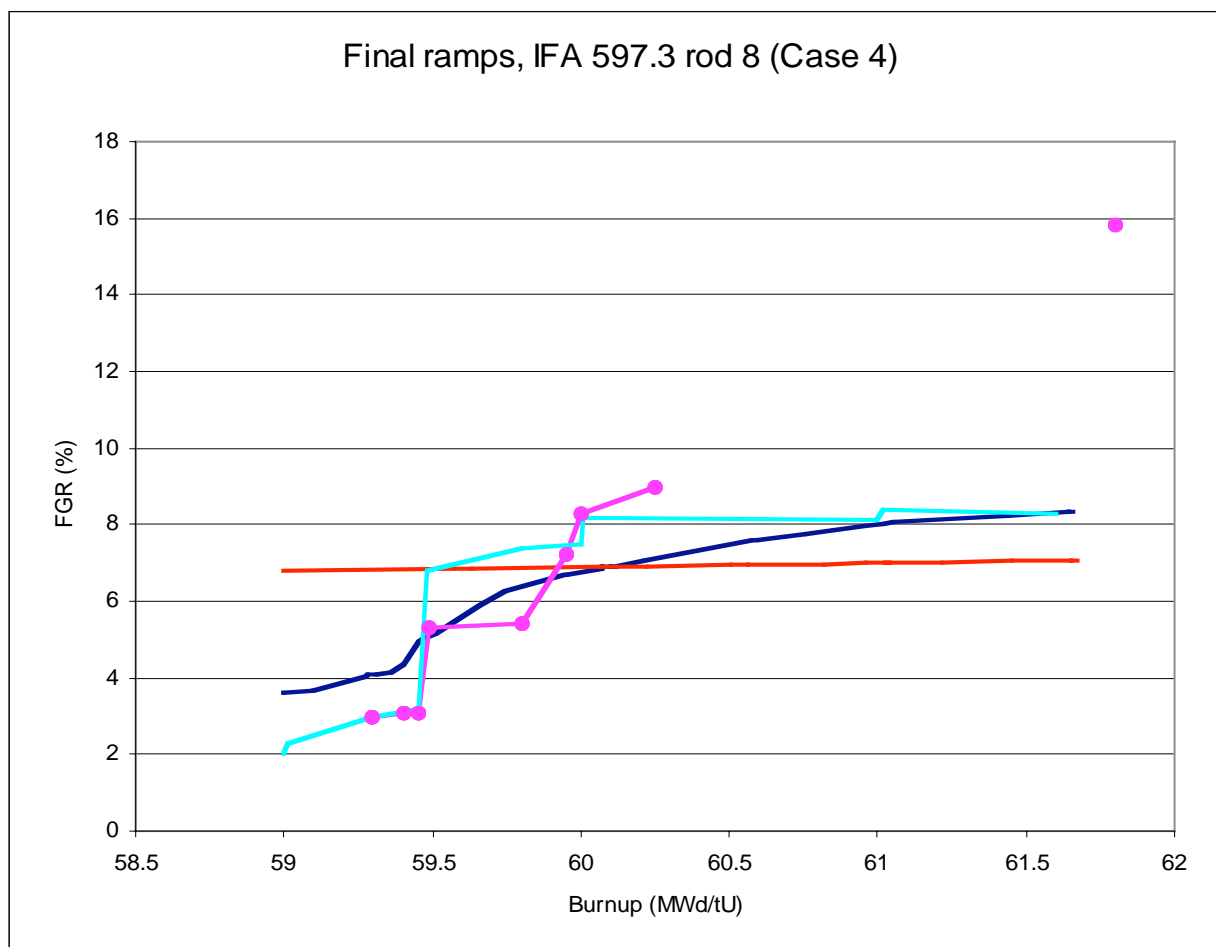
Typical code structure





FUMEX-2 Case 4 IFA-597.3

FGR calculated for rod 8 during 3rd loading

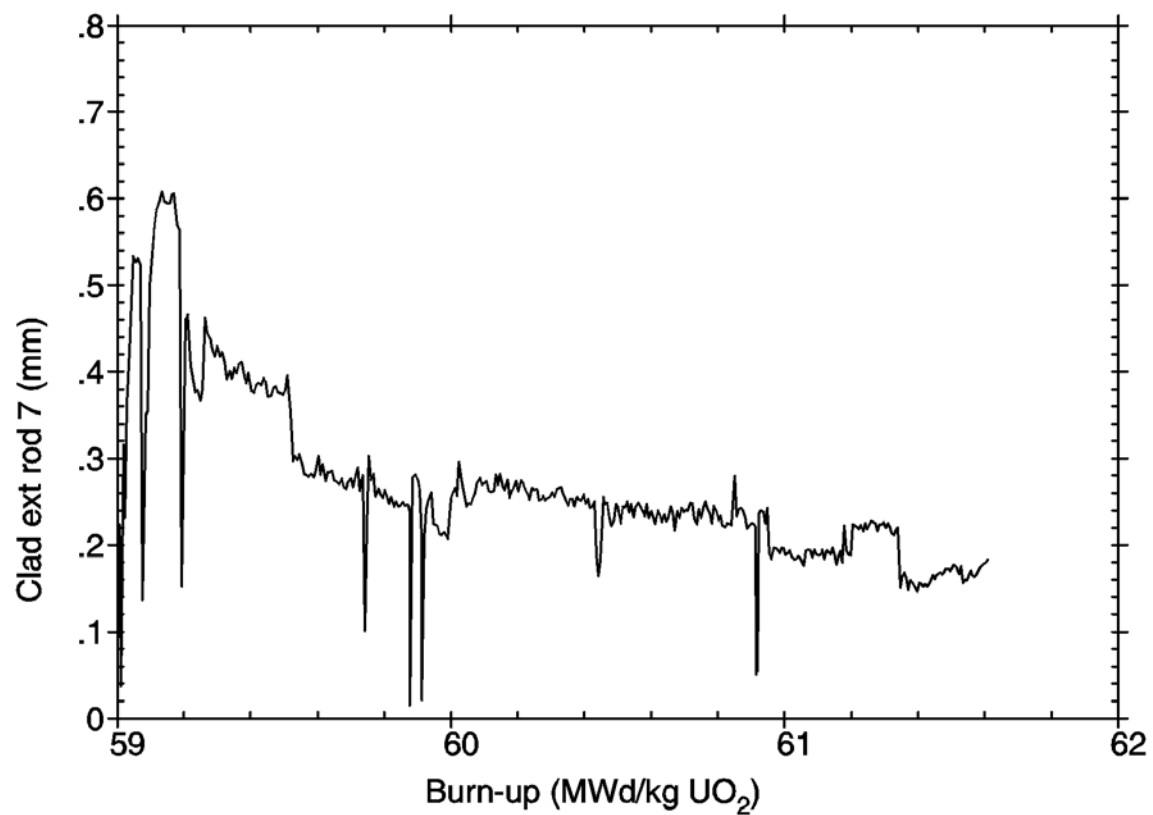


← PIE value = 15.8%



FUMEX-2 Case 3 IFA-597.3

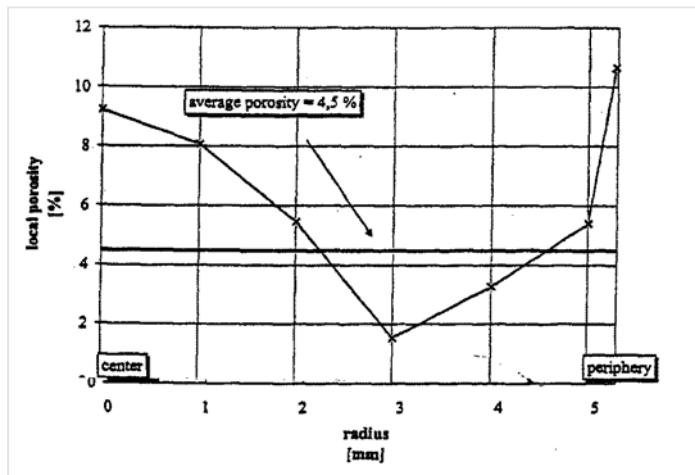
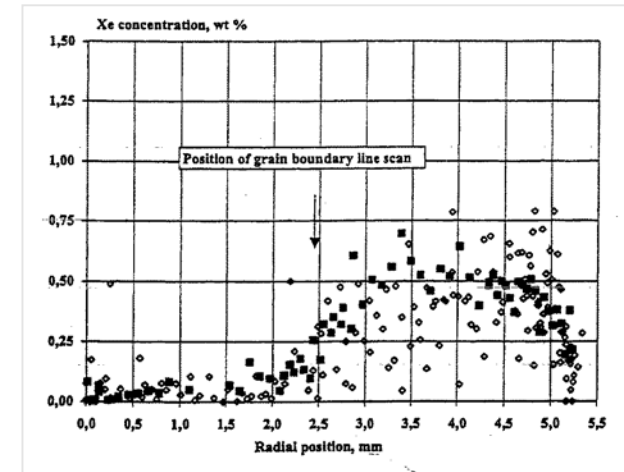
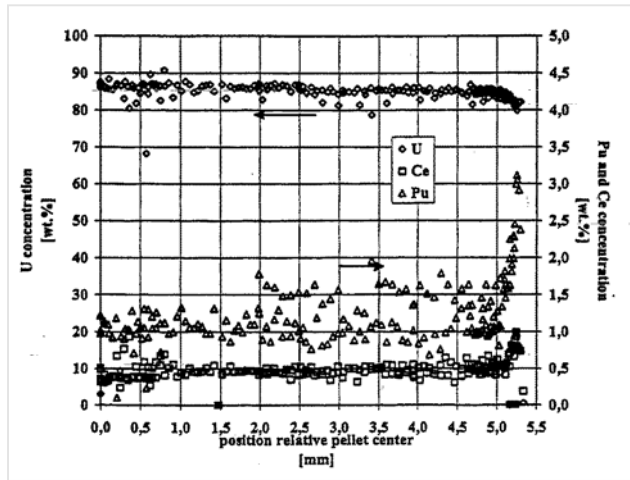
Clad elongation of rod 7 during 3rd loading





FUMEX-2 Case 4 IFA-597.3

Studsvik final PIE



EPMA profiles

Porosity distribution



Xenon distribution

38.8GWd/tU



Figure 3 : optical macroscopy of the sample.

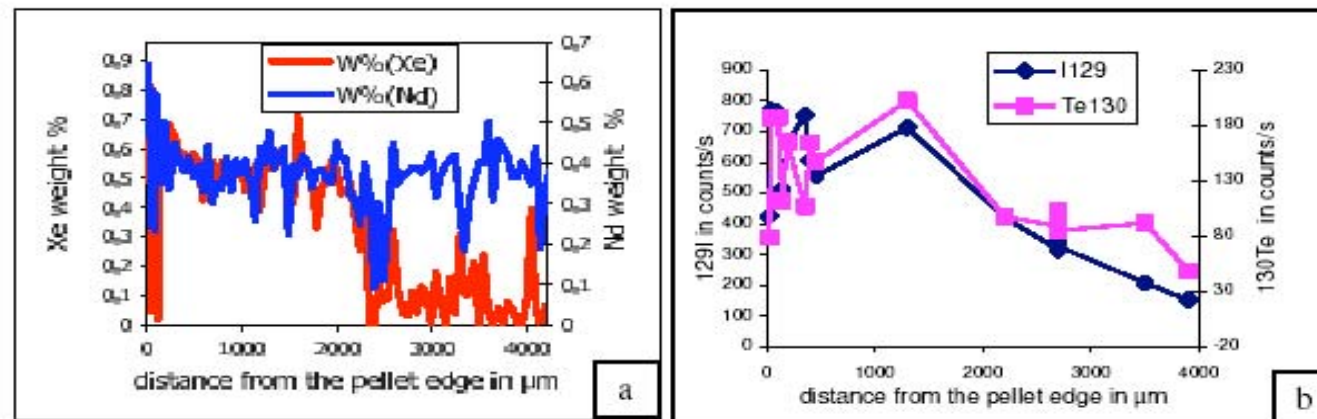


Figure 4 : EPMA quantitative concentration profile of xenon and neodymium (a) and SIMS profile of iodine and tellurium measured along the purple radius shown on figure 3.



“The xenon concentration measured by EPMA decreases at mid-radius to be nearly zero in the pellet centre. Xenon is known to be badly detected by EPMA when it forms bubbles with size bigger than a few tenth of micron [3].

The decrease of xenon must then not be understood as a xenon depletion but as a xenon precipitation in bubbles associated to some xenon release. The measured fraction of released gas is indeed only 3.8%, which is not consistent with a total xenon depletion in the pellet centre. This interpretation is consistent with the fuel microstructure observed by SEM”

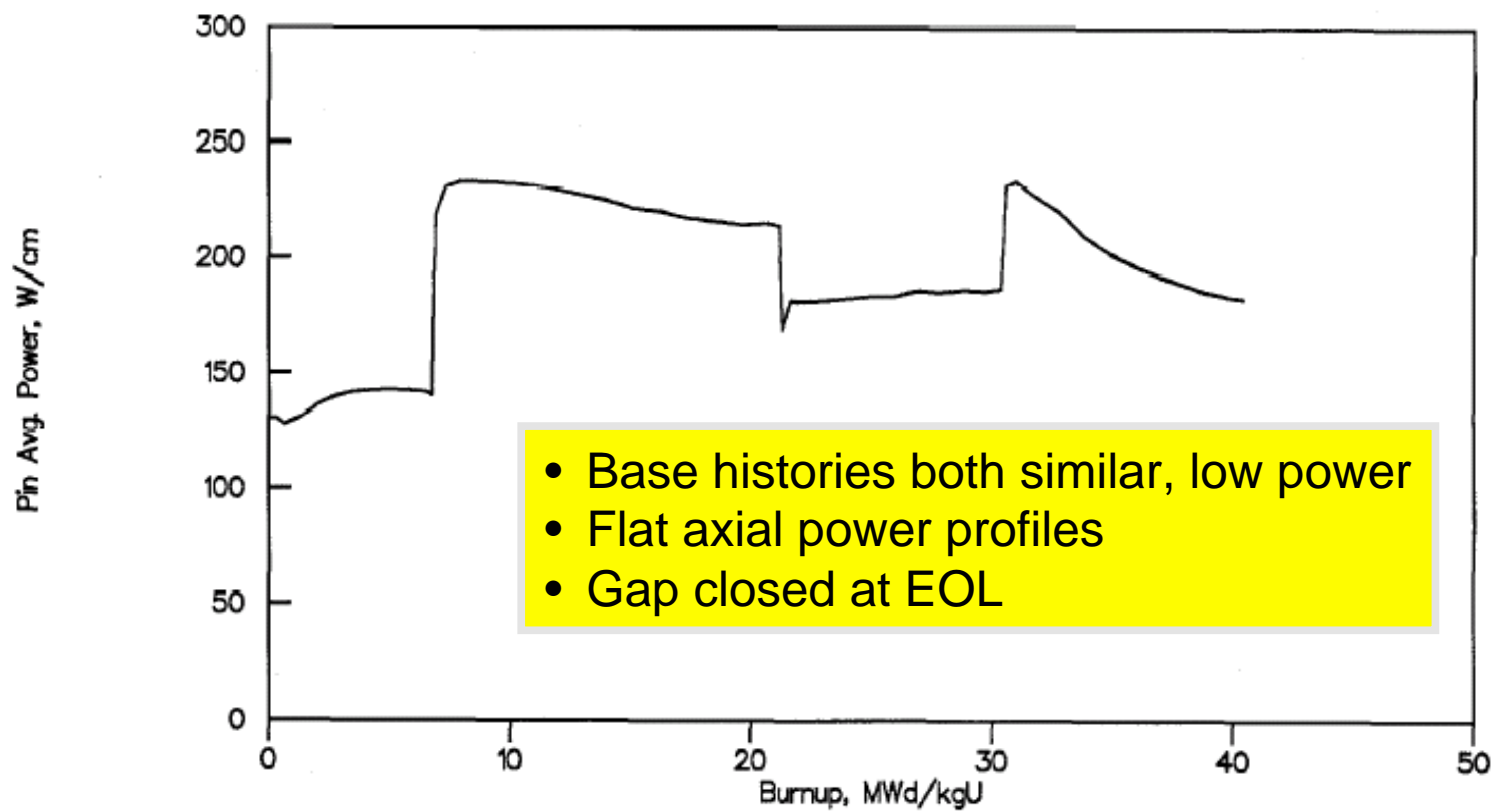


FUMEX-2 Cases 14 and 15 Risø-3 AN3 & AN4

- AN3 (35.6 MWd/kgUO₂)
 - re-filled with He, re-instrumented with TF & PF
 - FGR at EOL
 - Extensive PIE
- AN4 (35.6 MWd/kgUO₂)
 - re-filled with Xe, re-instrumented with TF & PF
 - FGR at EOL
 - Extensive PIE

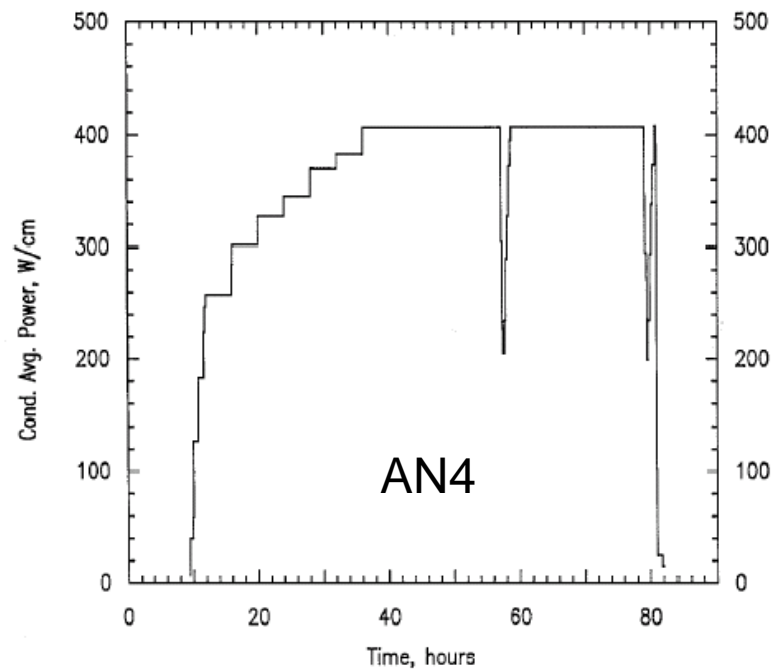
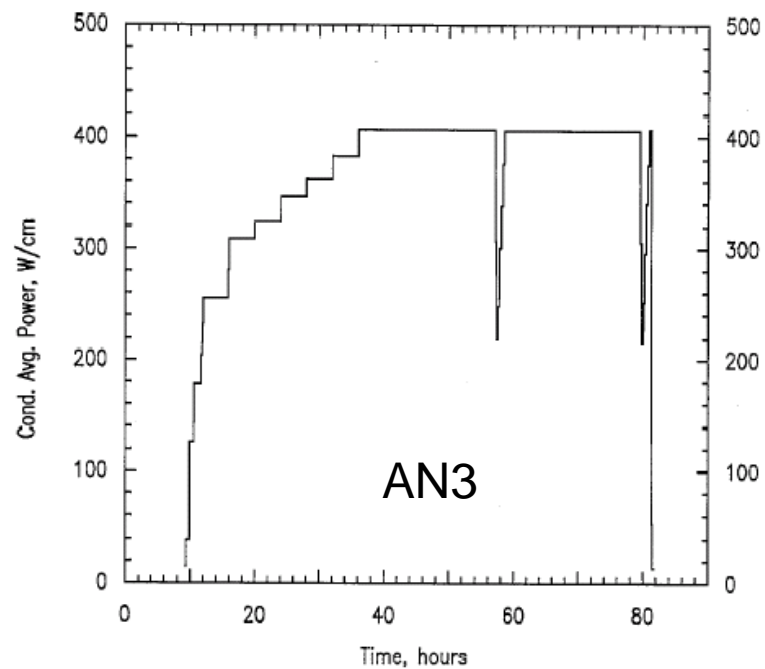


FUMEX-2 Cases 14 and 15 Risø-3 AN3 & AN4





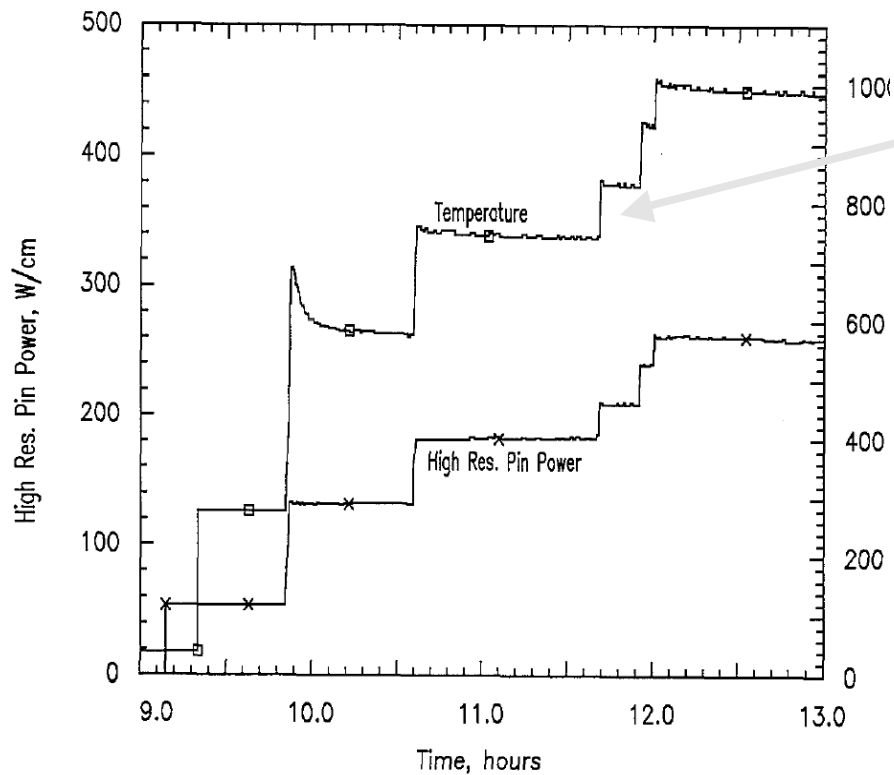
FUMEX-2 Cases 14 and 15 Risø-3 AN3 & AN4



Bump irradiation histories



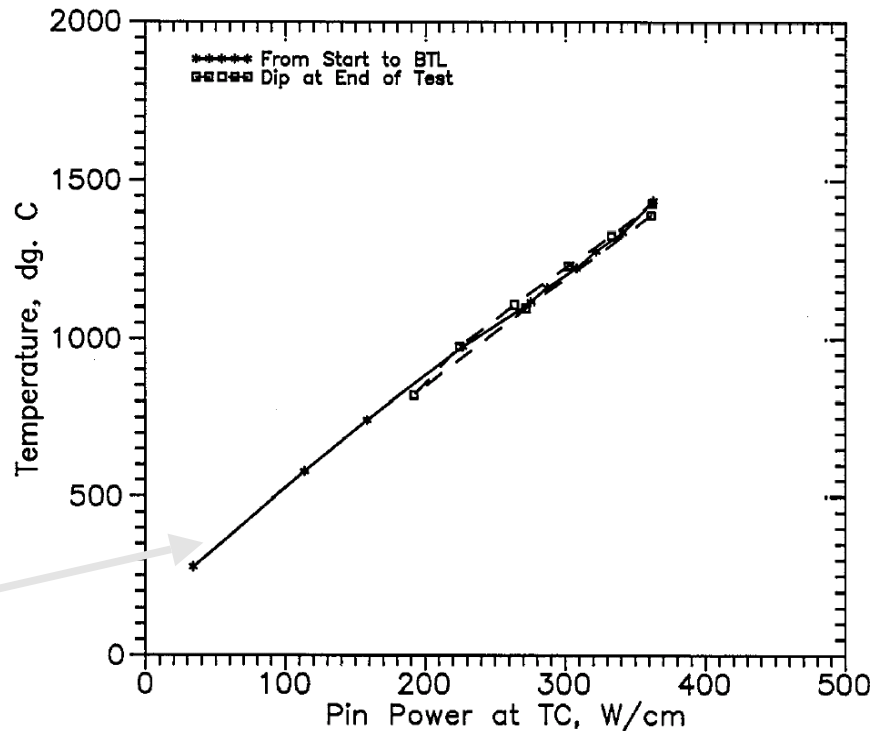
FUMEX-2 Cases 14 Risø-3 AN3



Temperature v time

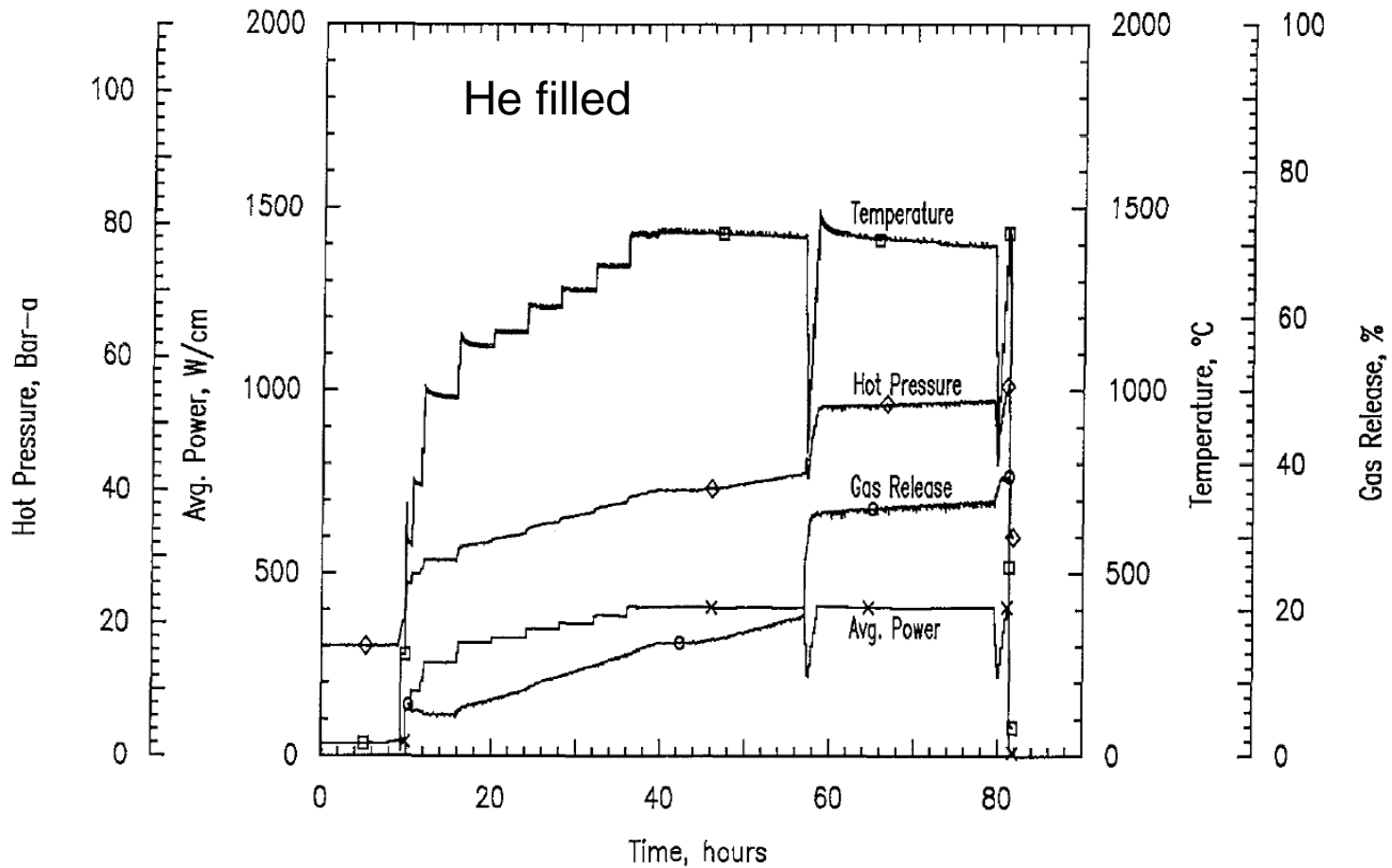
Temperature v power

- closed gap
- high burn-up





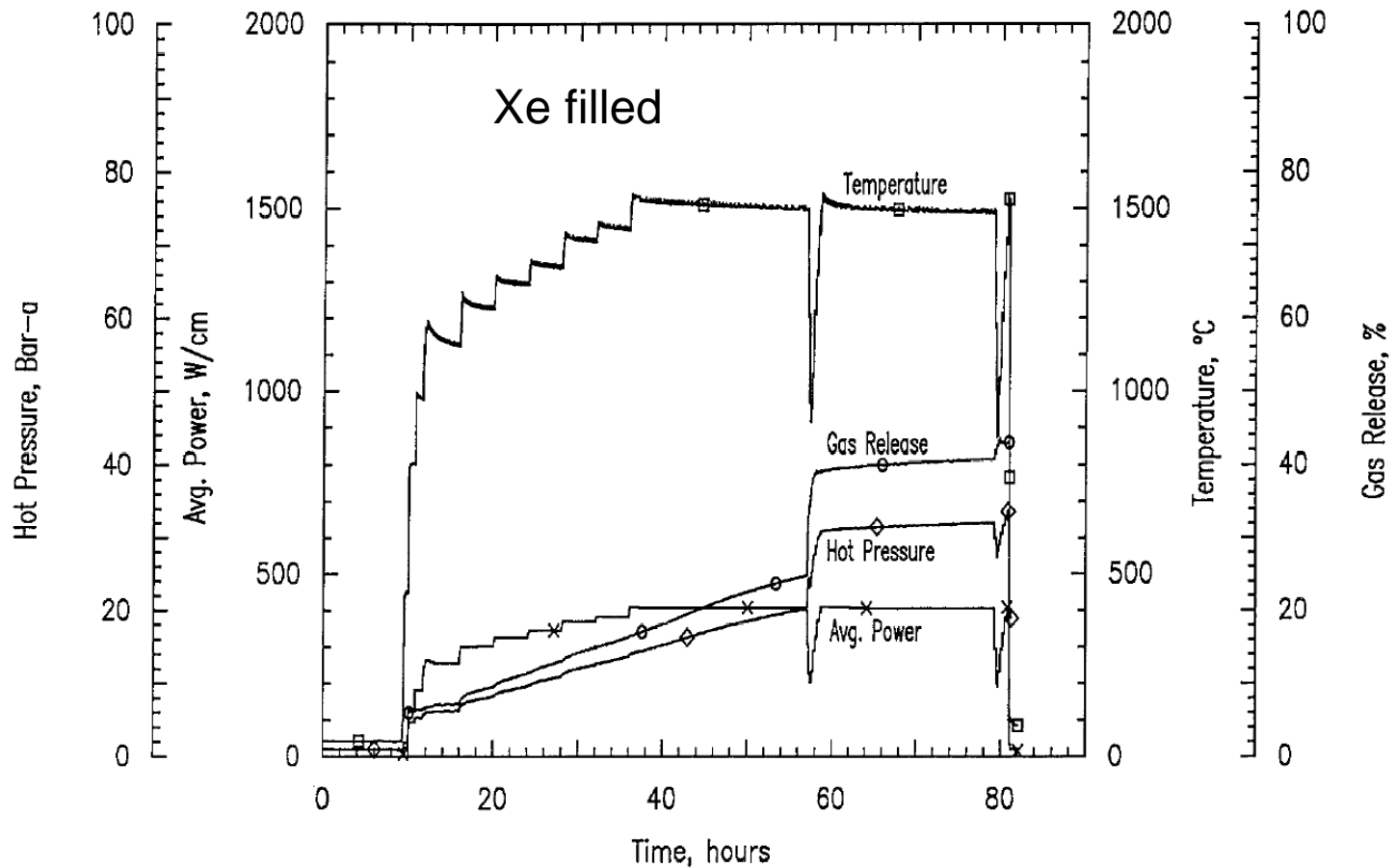
FUMEX-2 Cases 14 Risø-3 AN3



In-pile measurements



FUMEX-2 Cases 15 Risø-3 AN4

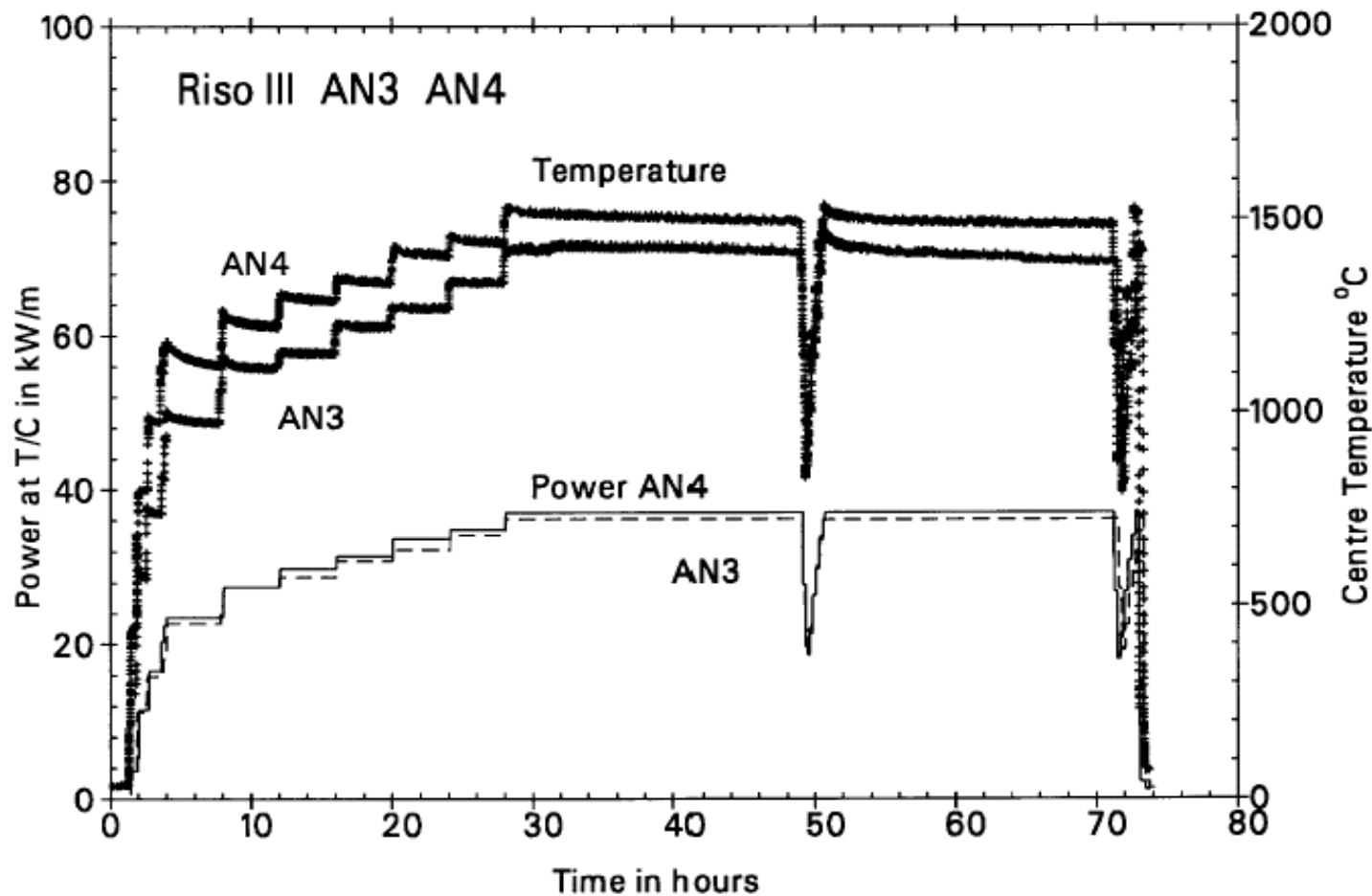


In-pile measurements



FUMEX-2 Cases 14 and 15

Risø-3 AN3 & AN4 comparison
The effect of fill gas composition in a closed gap

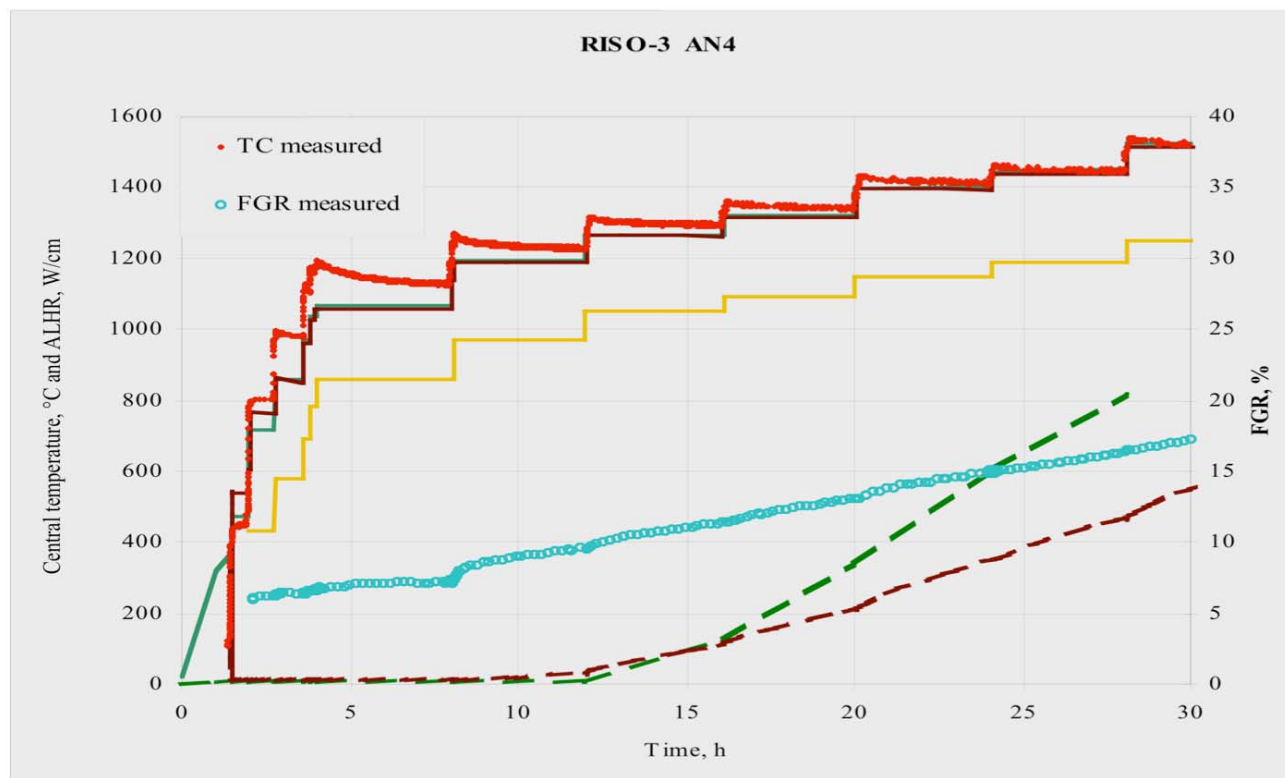


Burn-up = 35.74 MWd/tUO₂ AN3 (15 bar He) AN4 (1 bar Xe)



Temperature Modelling of Ramp Tests

Figure 2: Fuel centre temperature and fission gas release from the Risø AN4 ramp

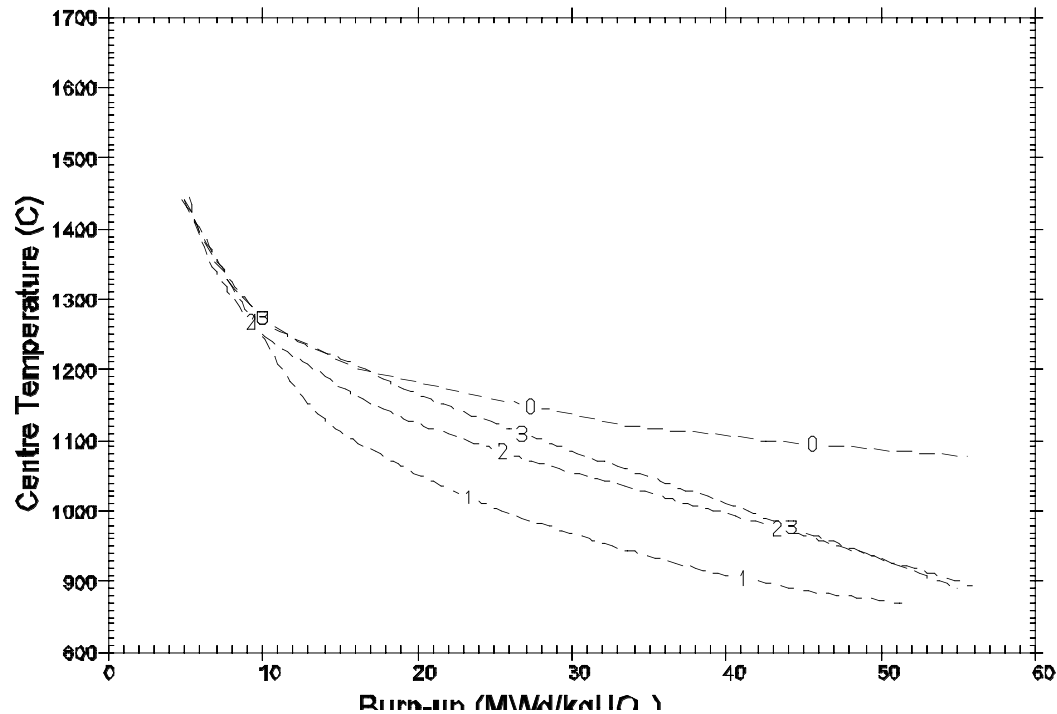


The majority of the codes follow the measured fuel centre temperature during the ramp quite well, the code prediction lying below the measurements is shown as an example of how choice of input parameters to a code can alter the predictions significantly, and with different input data this code can match the data much more closely. The two FGR predictions shown on the figure are also in good agreement with the end of test FGR. One feature of the Risø temperature ramps that was not modelled by any code was the temperature overshoot on each step during the rise to power.



FUMEX-2 Case 27, Simplified Power Histories

- 1 To define the locus of centreline temperature and burn-up satisfying the criterion for 1 % fission gas release.

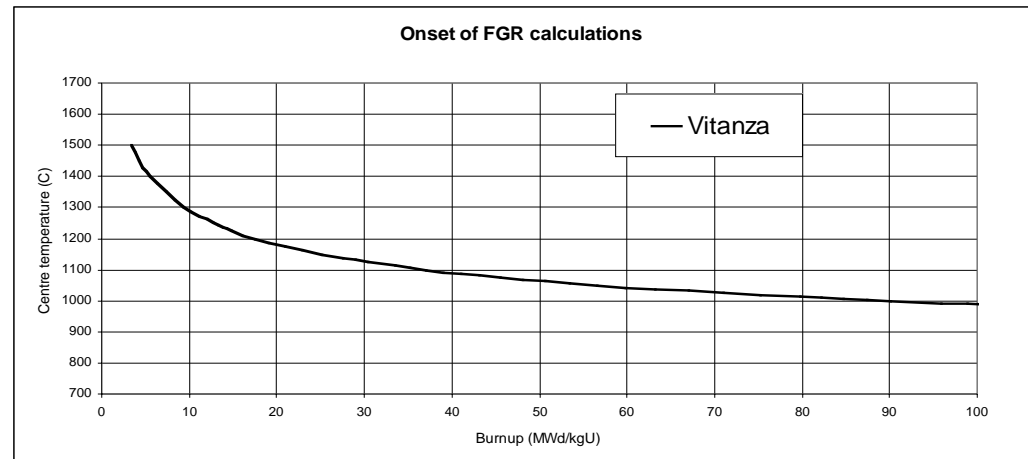


Possible loci for the 1% threshold using different modelling assumptions



Modelling the Vitanza Threshold

Case 27(1) asked the teams to reproduce the experimental result of a burnup dependent threshold centre temperature for Fission gas release (the Vitanza threshold) and extend their predictions to 100MWd/kgU. This empirical line was first developed from experimental data at the Halden Reactor Project and is widely used as an indicator of the conditions required for significant FGR (>1%).





Modelling the Vitanza Threshold

Case 27(1) There has been recent evidence that the Vitanza threshold is showing too high temperatures at high burnups where there is little data, and beyond the reasonable validation range of around 50MWd/kgU. What evidence that exists strongly suggests an enhancement of FGR at high burnup where a “rim effect” of enhanced porosity at the pellet surface has also developed.

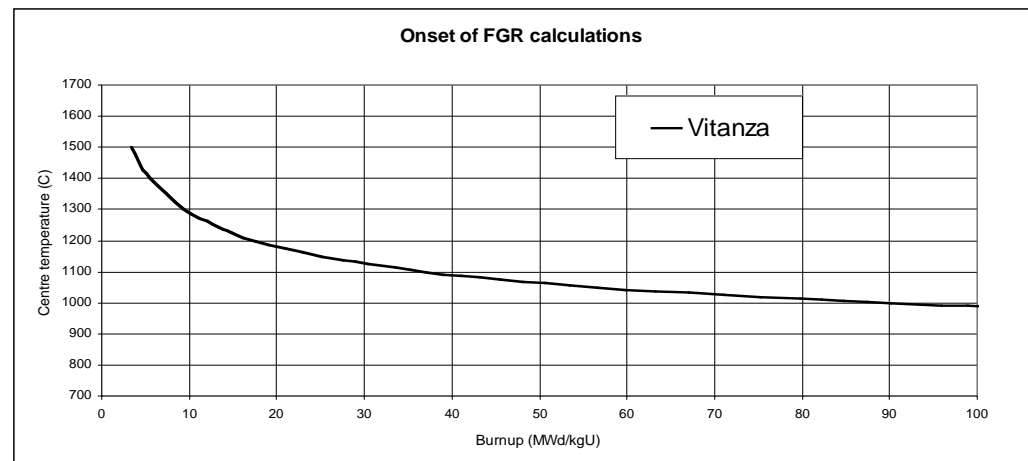
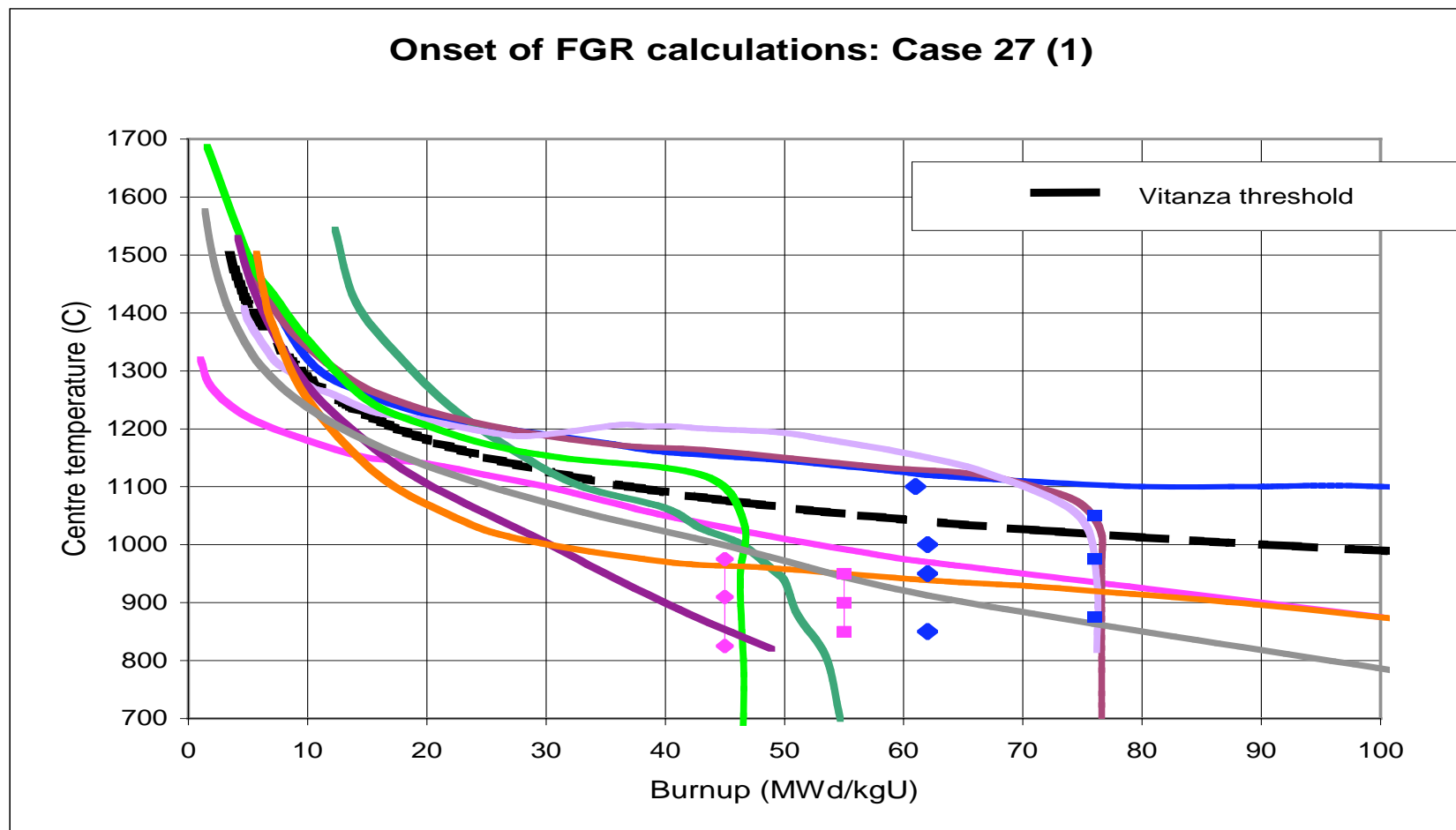




Figure 3: Modelling of the Vitanza Fission Gas Release Threshold



The first Figure gives some indication of the modelling difficulties encountered at high burnup. For many codes a FGR in excess of 1% is predicted, regardless of temperature at a burnup limit. This behaviour appears as a vertical line in the plot, and the points shown represent variations of modellers' assumptions to see where this limit might be.



Figure 4: Modelling of the Vitanza Fission Gas Release Threshold

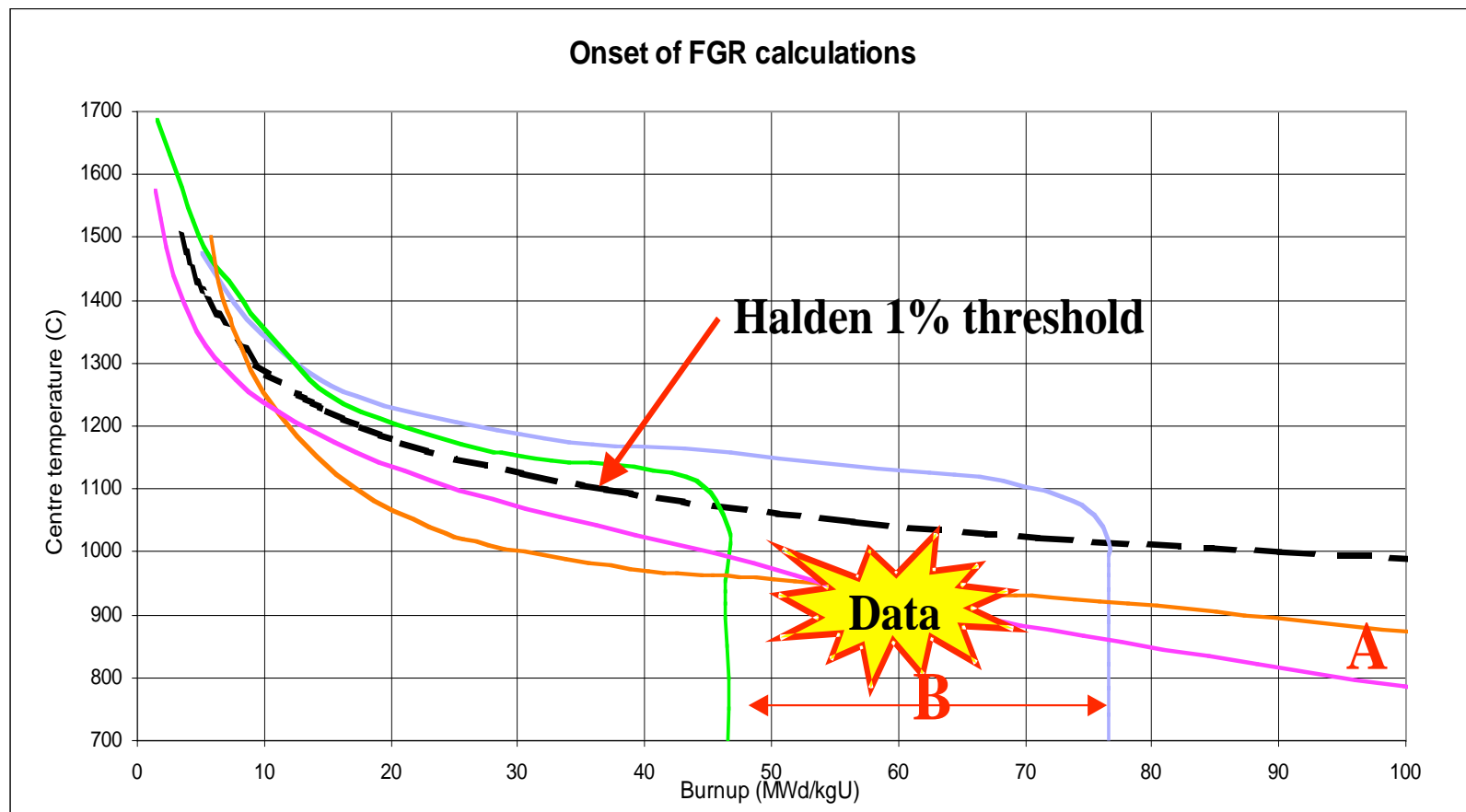
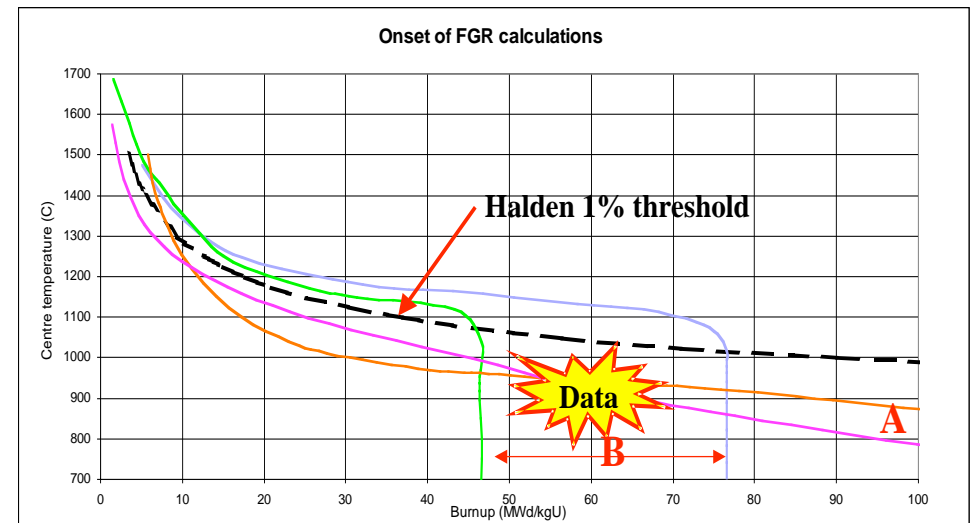


Figure (4) is a simplified version of Figure (3), highlighting the modelling trends and indicating where additional data would be useful in determining what effects are actually occurring at these high burnups.



Modelling the Vitanza Threshold

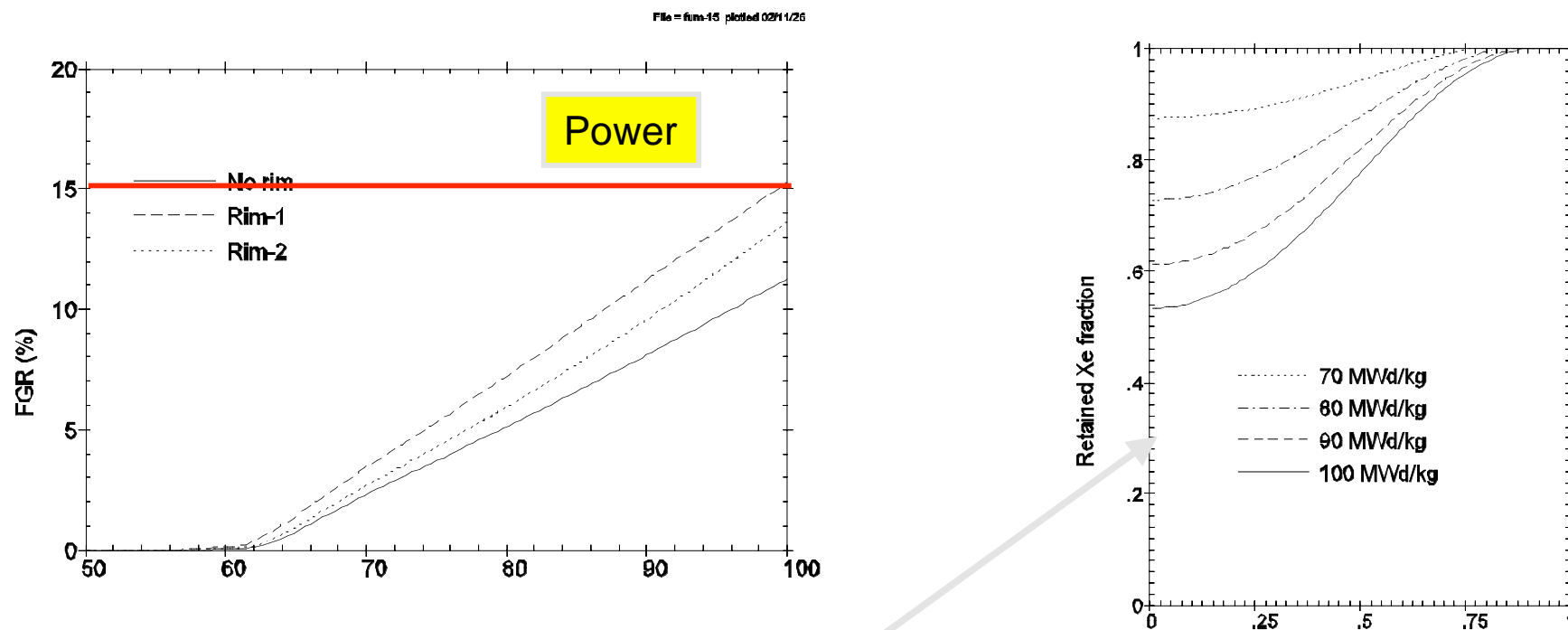
The two general trends A and B shown in the Figure 4 are a result of high burnup modelling assumptions. Where the modelling has a burnup dependence of diffusion parameters, or a saturation effect, an effectively continuous extrapolation of the existing Vitanza curve is seen, this is type A behaviour. Where release is assumed to come from a restructured region, the type B behaviour is found, and significant release is initiated at a burnup limit, with little temperature dependence.





FUMEX-2 Case 27, Simplified Power Histories

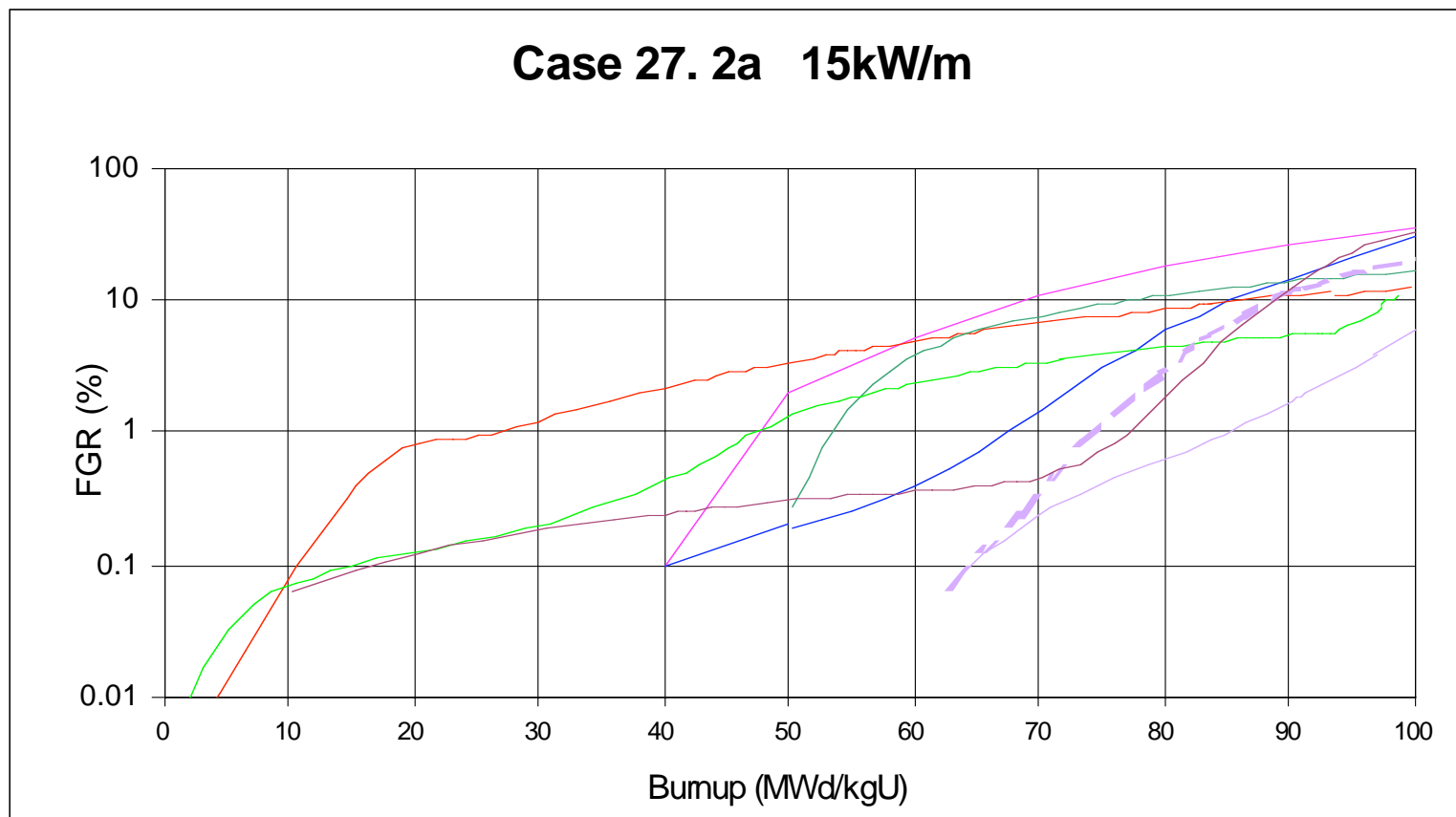
2a) for a constant power of 15 kW/m from BOL to 100 MWd/kgU.



Retained xenon at different levels of burn-up



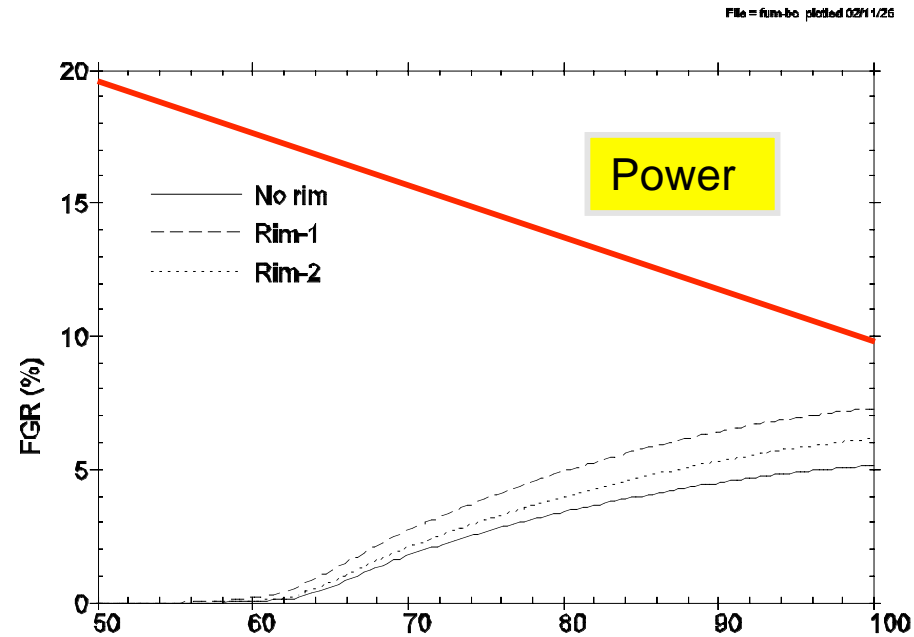
“Fuel modelling is a mature science”





FUMEX-2 Case 27, Simplified Power Histories

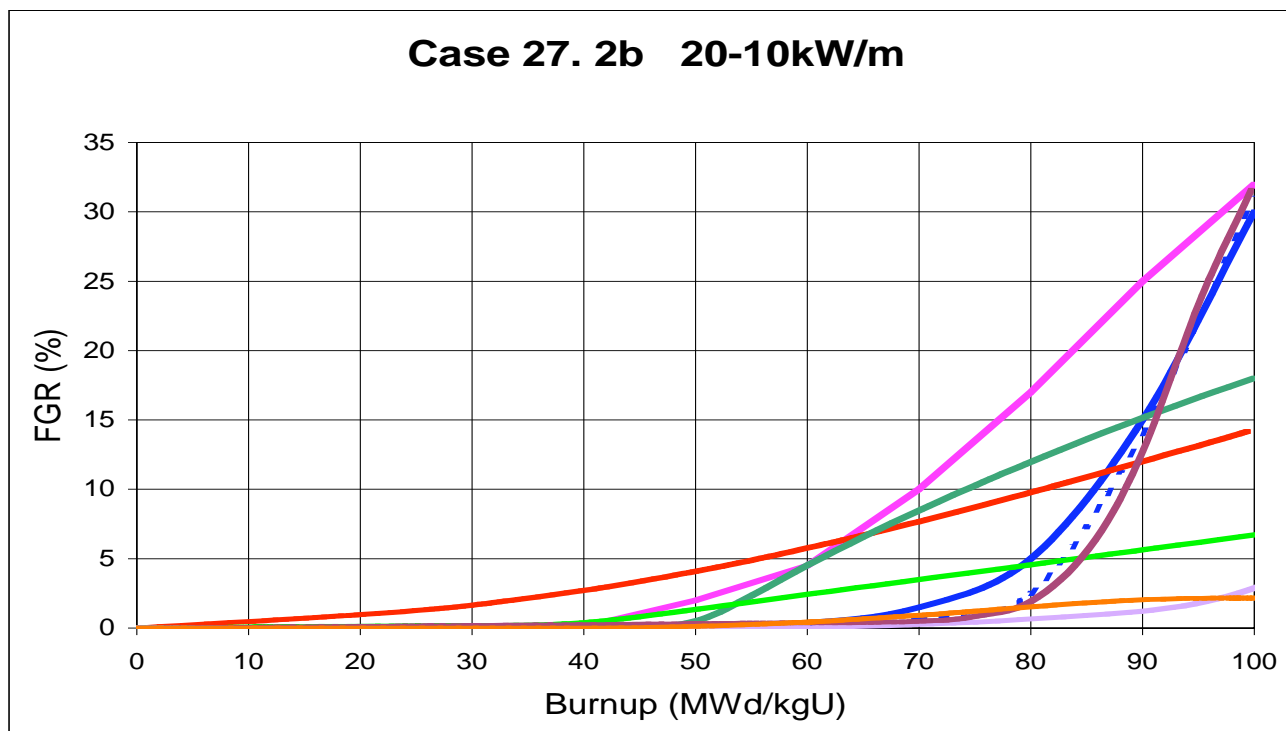
2b) linearly reducing power from 20 kW/m at BOL to 10 kW/m at 100 MWd/kgU.





“Fuel modelling is a mature science”

Figure 6: Case 27.2b. Idealised power history, reducing power from 20kW/m to 10kW/m



A selection of the calculated results for the fission gas release from the simplified case 27.2b is shown.

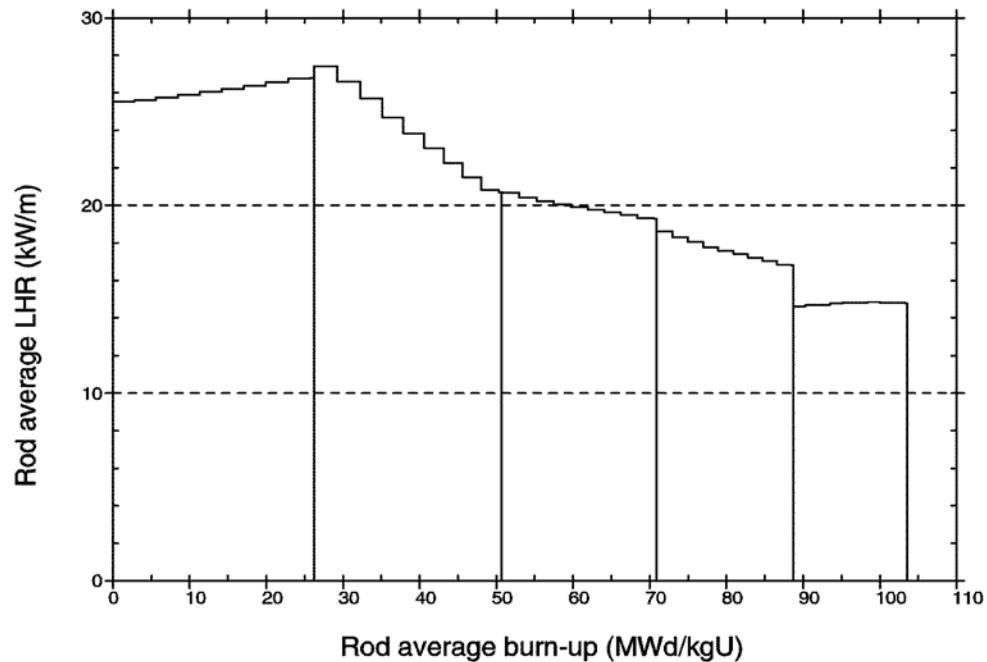
The codes give a very wide range of predictions for the histories, which are designed to challenge high burnup predictive capability. The codes generally predict low FGR below 1% for normal burnups, to 50MWd/kgU, but at higher burnups the predictions vary, in a similar manner as seen for Case 27 (1).

Codes that model release from a rim or gas saturated region tend to give the highest FGR at extremely high burnups.



FUMEX-2 Case 27, Simplified Power Histories

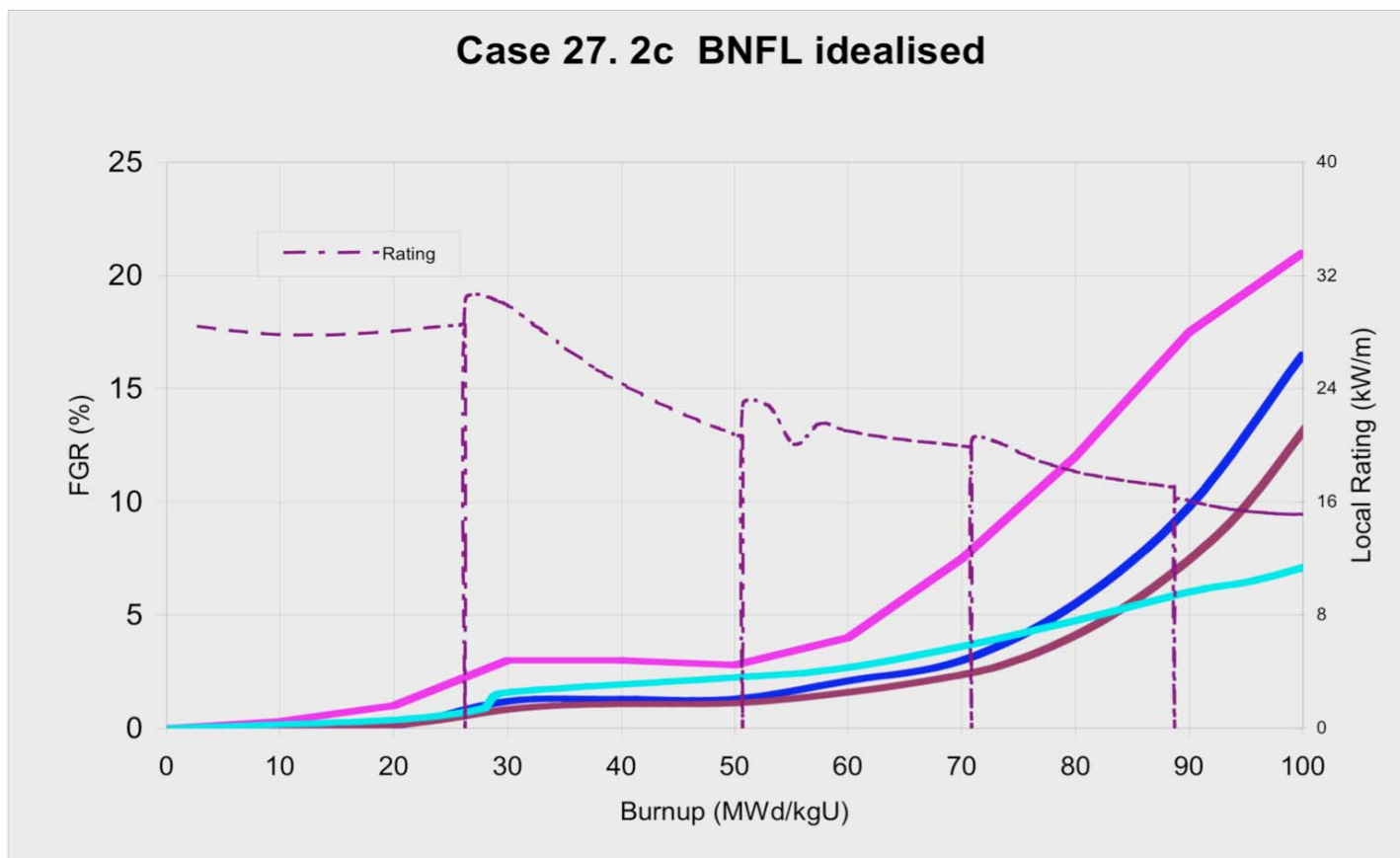
2c) notional history supplied by BNFL



- 2800 MWth W 3 loop PWR
- 17x17 assembly design
- 5 cycle irradiation
 - 104 MWd/kgU
- Standard ADU UO₂ pellet
 - 50 micron mli grain size
- Advanced Zr cladding
 - model as standard Zr with no corrosion through life



Figure 7: Case 27 (2c): Fission gas release predictions for an idealised operational history to 100MWd/kgU provided by BNFL. The rating history of a single axial zone is given.



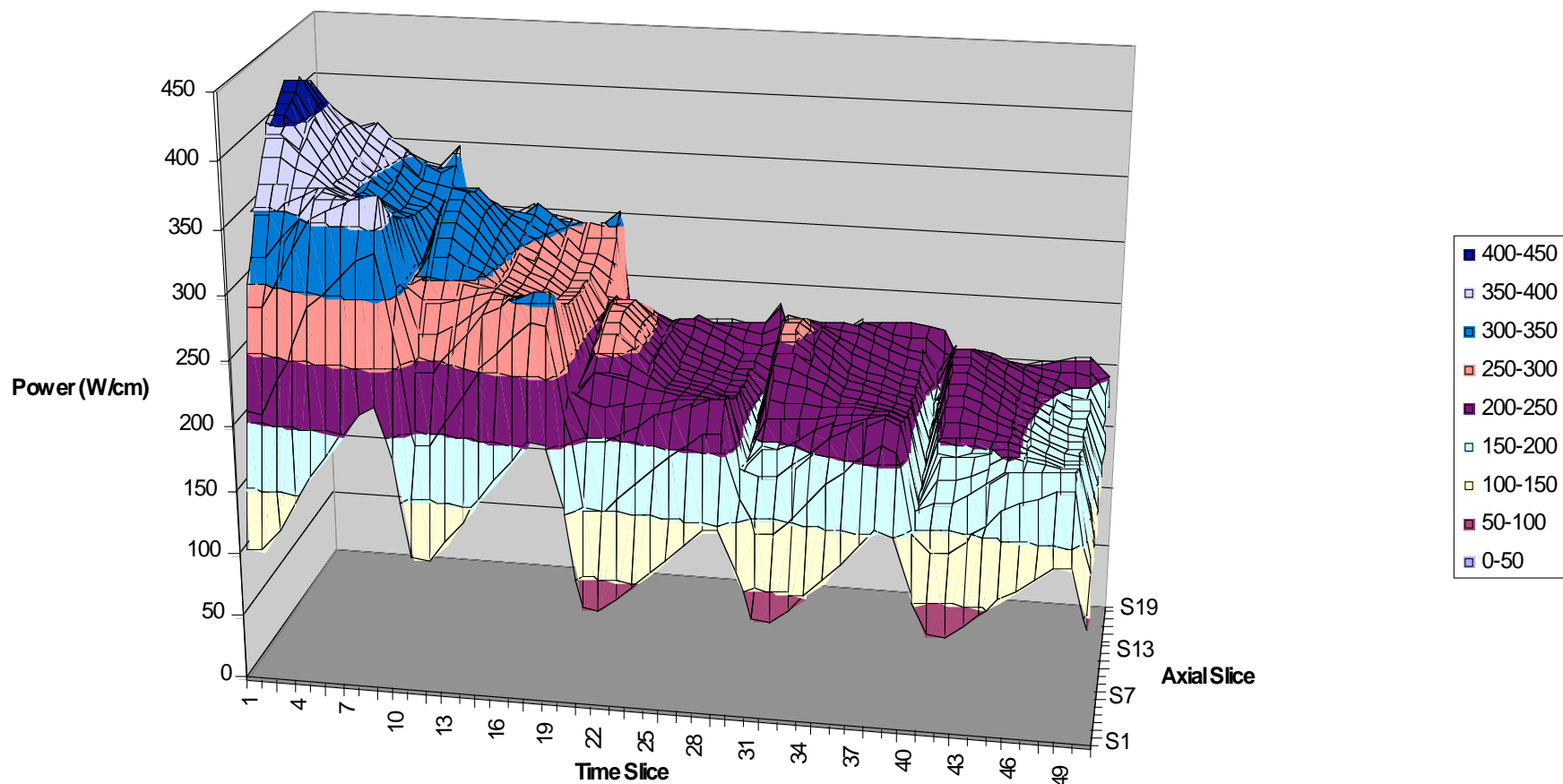
The notional history was provided by BNFL, the actual case was a 12 axial zone history with a final rod average burnup of 103MWd/kgU. The predictions shown in the figure are typical of the results achieved, and show low levels of FGR predicted at normal burnup, up to around 60MWd/kgU. However, despite a drop in power as burnup proceeds, the FGR is expected to increase significantly at the higher burnups.



FUMEX-2 Case 27, Simplified Power Histories

2d) idealized case supplied by FANP

Power History for 5 Cycles
New Cycle at Time Slice 12, 22, 32, 42
Rod Bottom at Axial Slice R1





FUMEX-2 Case 27, Simplified Power Histories

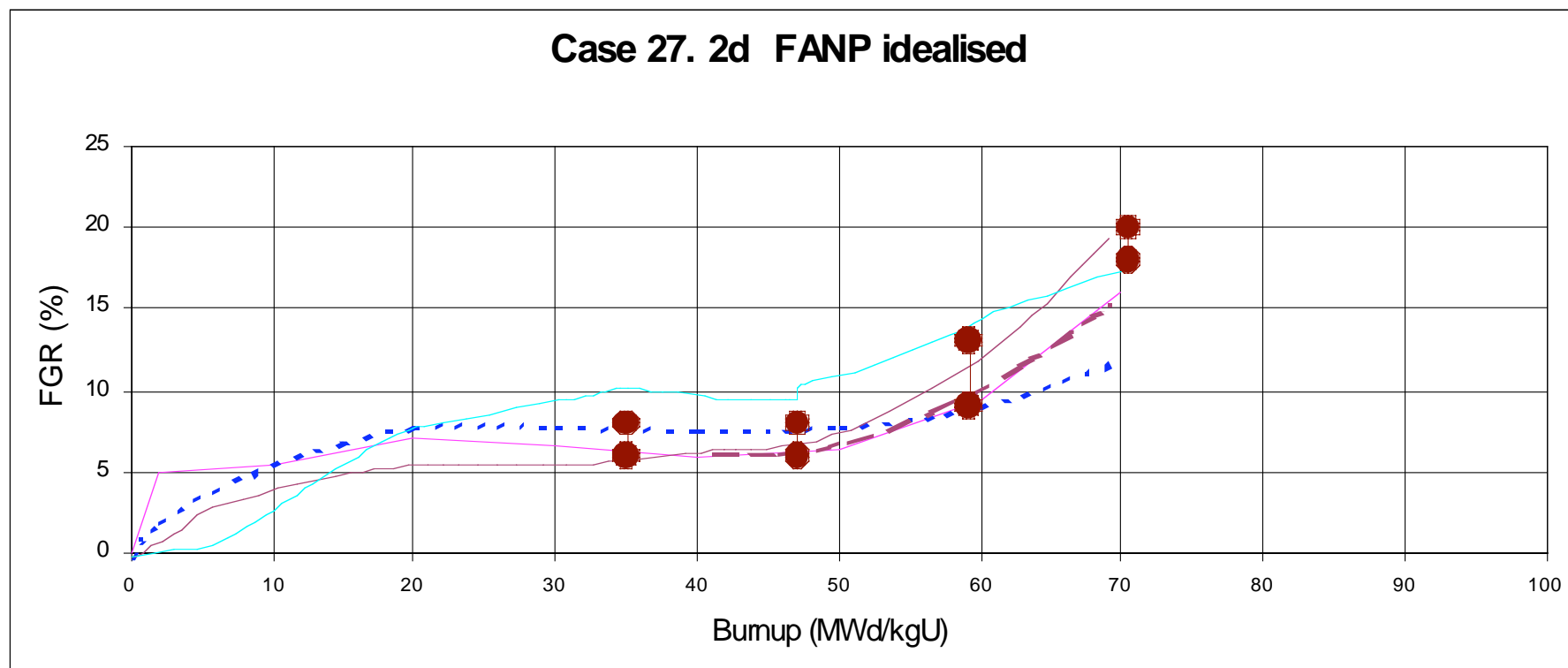
2d) idealized case supplied by FANP

- 15x15 design, modern PWR
 - 22 bar helium fill gas
 - 49 step 12 zone history to 70 MWd/kg
- standard UO₂ pellet
 - 4% enriched
 - 10 micron mli grain size
 - low densification
- Low corrosion Zr-4 cladding
 - standard creepdown
- FGR data:

End of cycle	Full power days	Measured FGR (%)
2	673.7	6 – 8
3	1007.3	6 – 8
4	1349.0	9 – 13
5	1689.8	18 – 20



Figure 8: Case 27 (2d) The fission gas indicated is representative of FANP fuel behaviour



The history provided by FANP (now Areva) was rather onerous at low burnups, and did not extend to an extreme burnup. This case was provided with details of the expected range of FGR up to 70 MWd/kgU, and it is good to see that the codes tended to give a good representation of the release, showing excellent agreement up to 60MWd/kgU, and still giving good agreement at 70MWd/kgU. Due to the power history in this case, it seemed to be less sensitive to details of the high burnup modelling, the majority of the FGR was well described by normal models and significant release occurred at low burnups.



Modelling of the mechanical interaction between the pellet and the cladding

- There is no consensus on a single way of modelling PCI, as the underlying mechanisms are not clearly defined.
- The new cladding materials need to be checked for PCI performance
- The models for PCI are still in a development stage and need validation



Modelling of the mechanical interaction between the pellet and the cladding

- A wide variety of modelling approaches are used, including pellet cracking, interface bonding, fission gas swelling, localised clad hydriding and the rim layer effect.
- The modelling techniques used include 1-D, 2-D and 3-D finite element modelling and various approximations to speed the analysis.



PCI

Experimental results

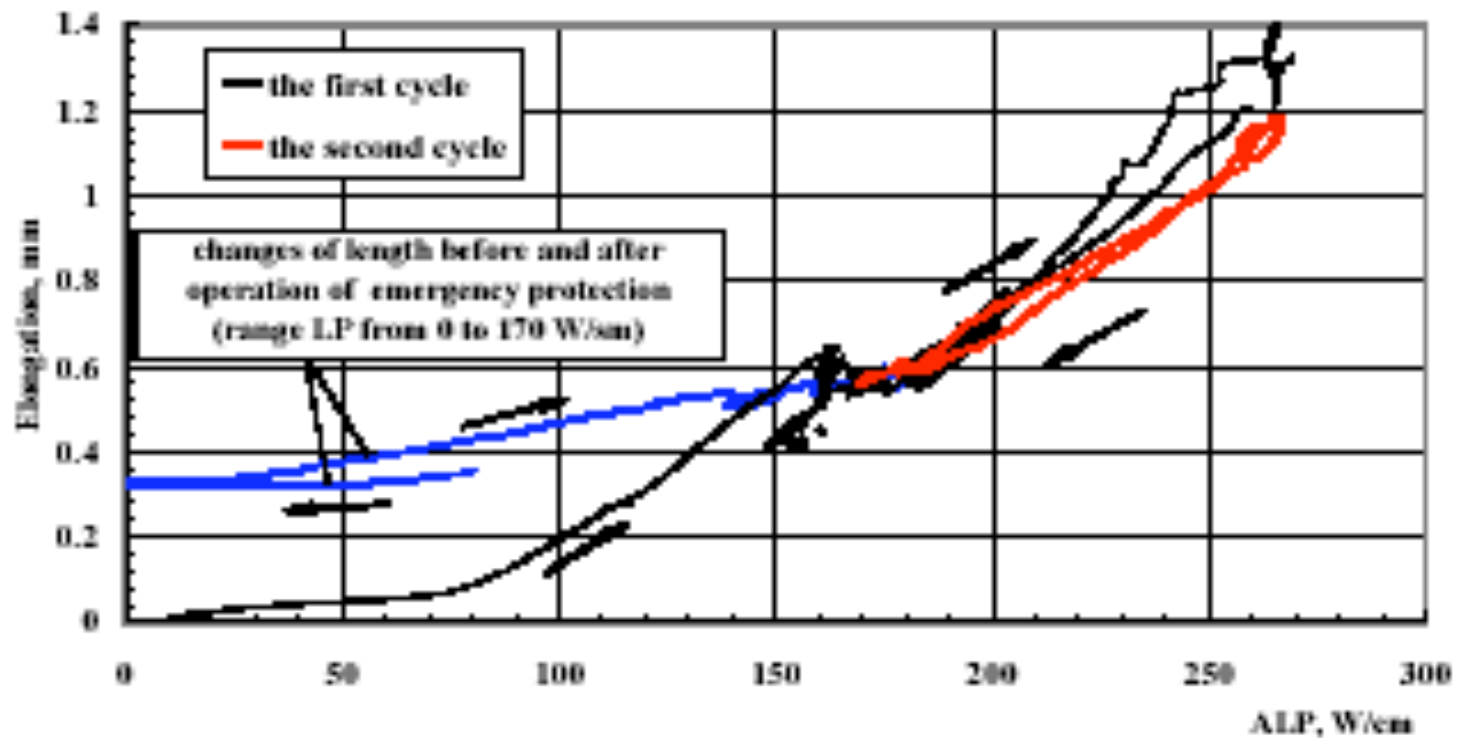
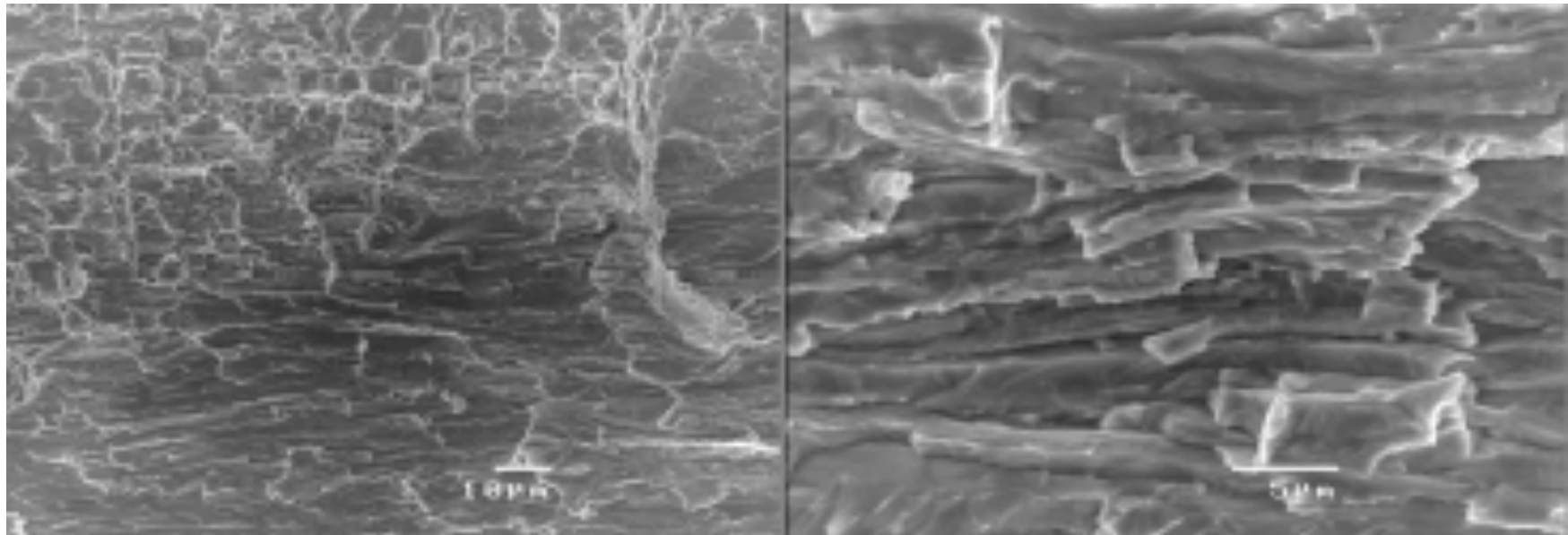


Fig. 4 – Change of the R75 fuel rod length as a function of average LP



PCI

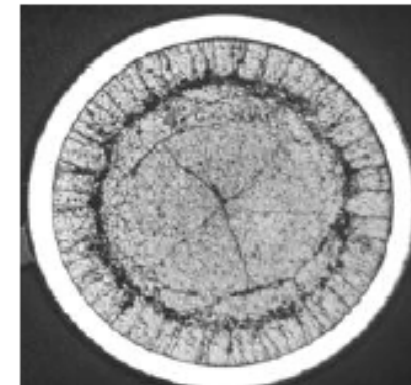
- Detailed metallography of cracking



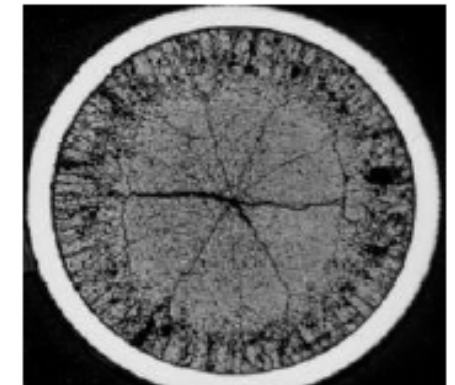


PCI

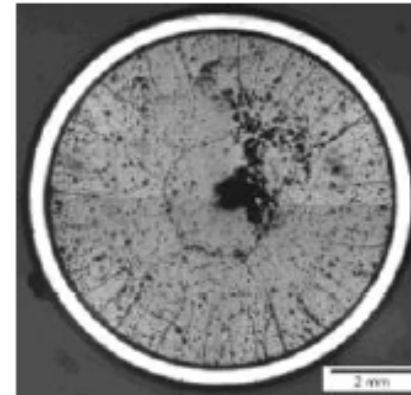
- Images from the Chromia doped fuel tests in France



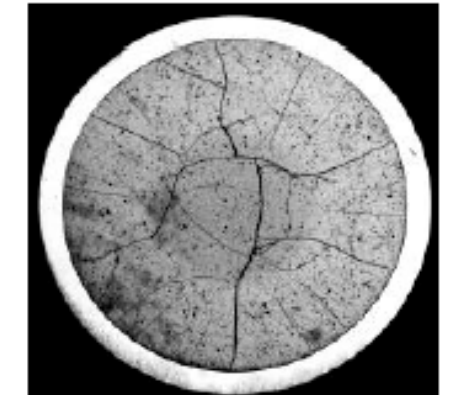
Section A from rodlet n°1 (47 kW/m)



Section D from rodlet n°2 (54 kW/m)

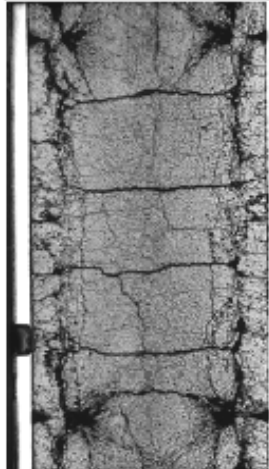


Section B from rodlet n°1 (40 kW/m)
Low power area

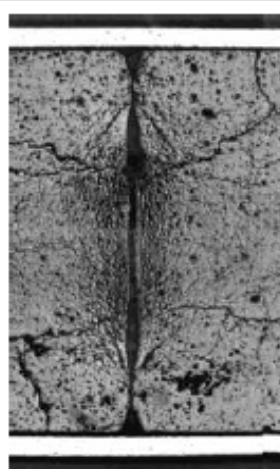


Section from rodlet n°4 (undoped)
Maximum power area 40 kW/m

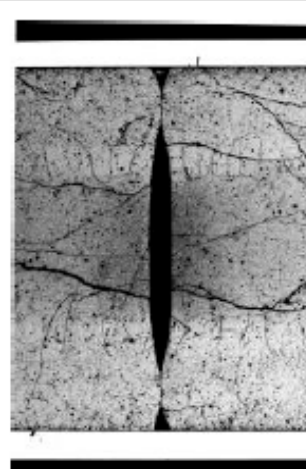
Figure 9 : comparison of cross- sections between doped and undoped fuel at different local power



Section B from rodlet n°1
Max. power area 47 kW/m



Section B from rodlet n°1
Low power area 40 kW/m



Section from rodlet n°4 (undoped)
Maximum power area 40 kW/m

Figure 10 : comparison of dshtags filling on longitudinal sections between doped and undoped fuel



PCI

Finite element analysis

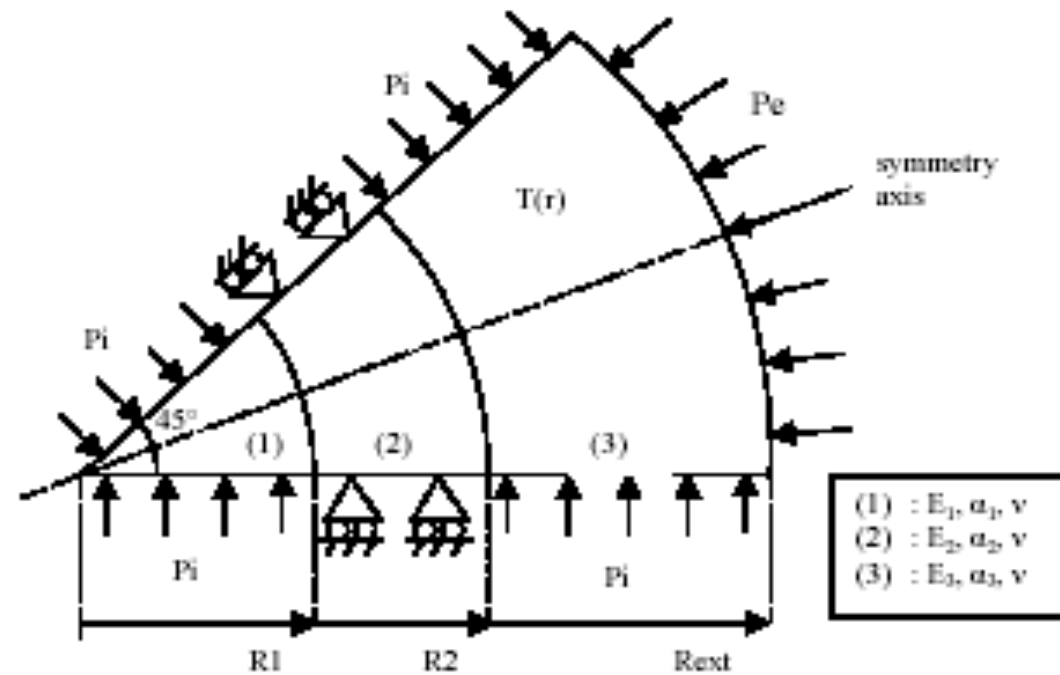


Figure 6: 2D modelling of a fragment for pellet-cladding contact case



PCI

- Detailed, multi-dimensional modelling of stress and atomic defects

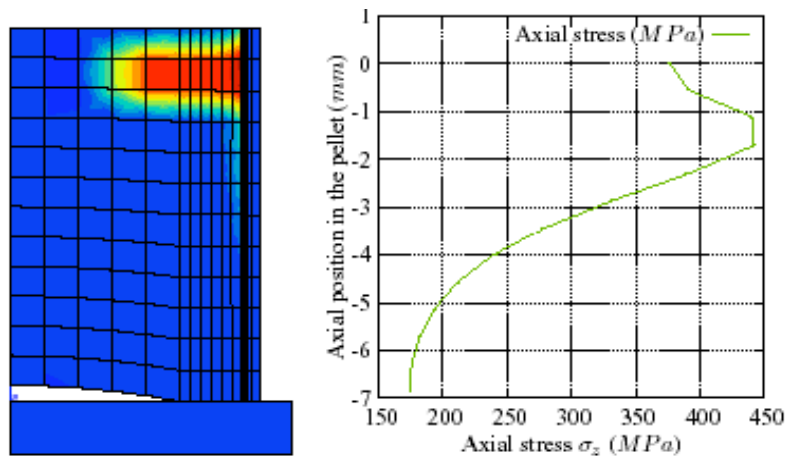


FIGURE 7 : Damage localisation in the (\bar{r}, \bar{z}) plane and consistency with three dimensional thermo-elastic axial stress calculation on the outer pellet face.

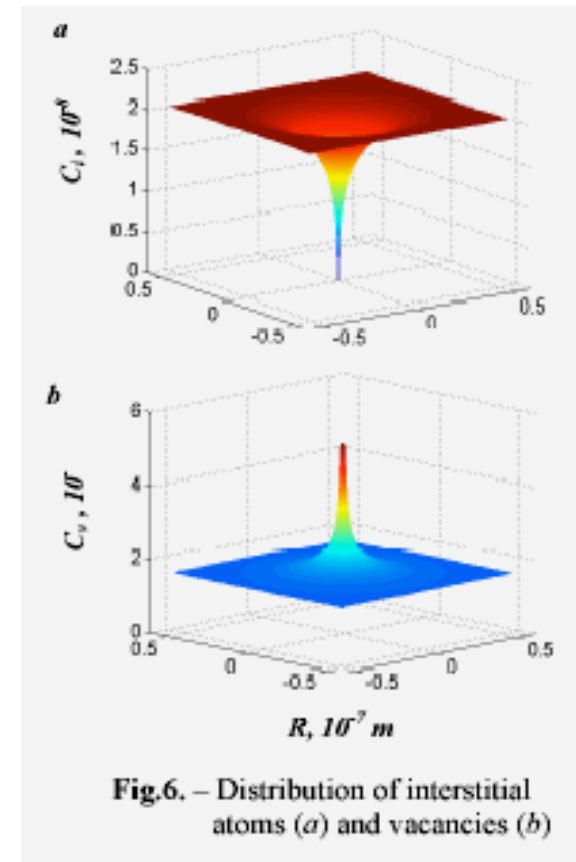


Fig.6. – Distribution of interstitial atoms (a) and vacancies (b)



High Burnup Approaches

The important feature of the experimental data that is informing the modelling, is that there is enhanced fission gas release at high burnup, compared with that expected using conventional modelling assumptions.

Three main approaches to deal with the high burnup effect have been used by the modelling teams:

- Contribution of FGR from the pellet rim – release from the restructured region
 - Magnitude of the effect was variable
- Burnup dependent diffusion parameters
 - Diffusion coefficient
 - Irradiation induced re-solution
- Limiting saturation concentration of gas in the UO_2 matrix.

In the majority of cases, explicit consideration was also taken for the thermal effect of the rim porosity.

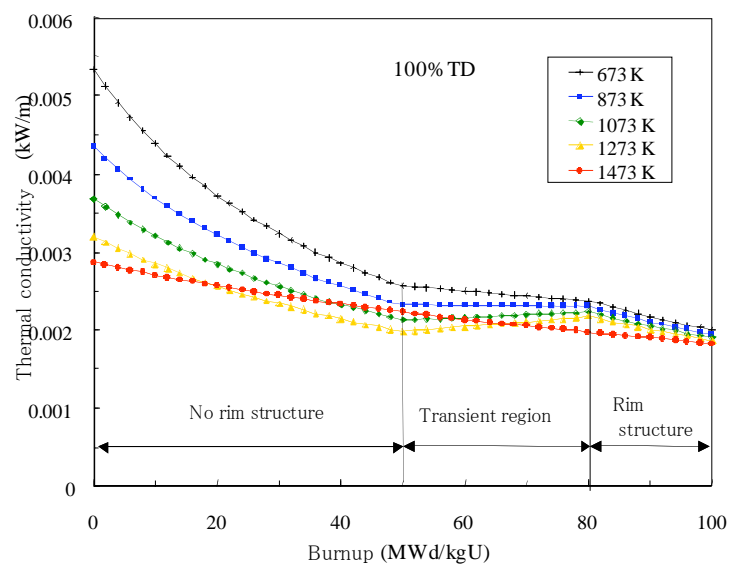




High burn-up Fuel

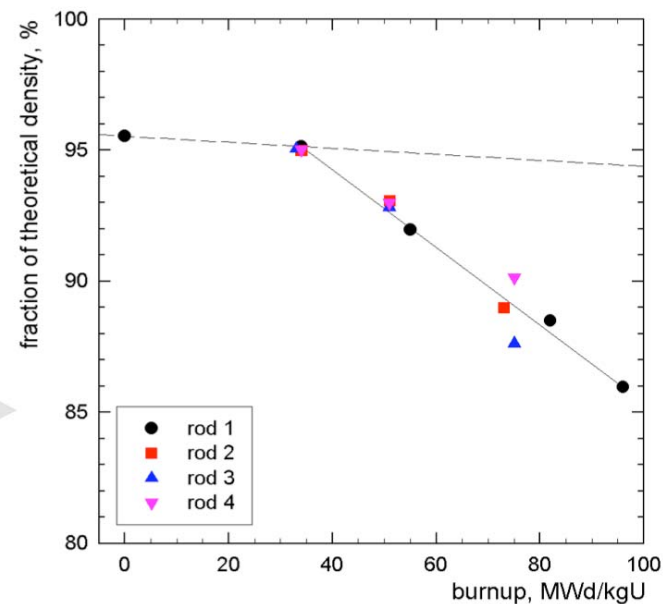
Some recent results from the HBRP

Kinoshita et al, ANS Orlando Florida September 2004



Effect of HBS on thermal conductivity

Effect of HBS on density/swelling

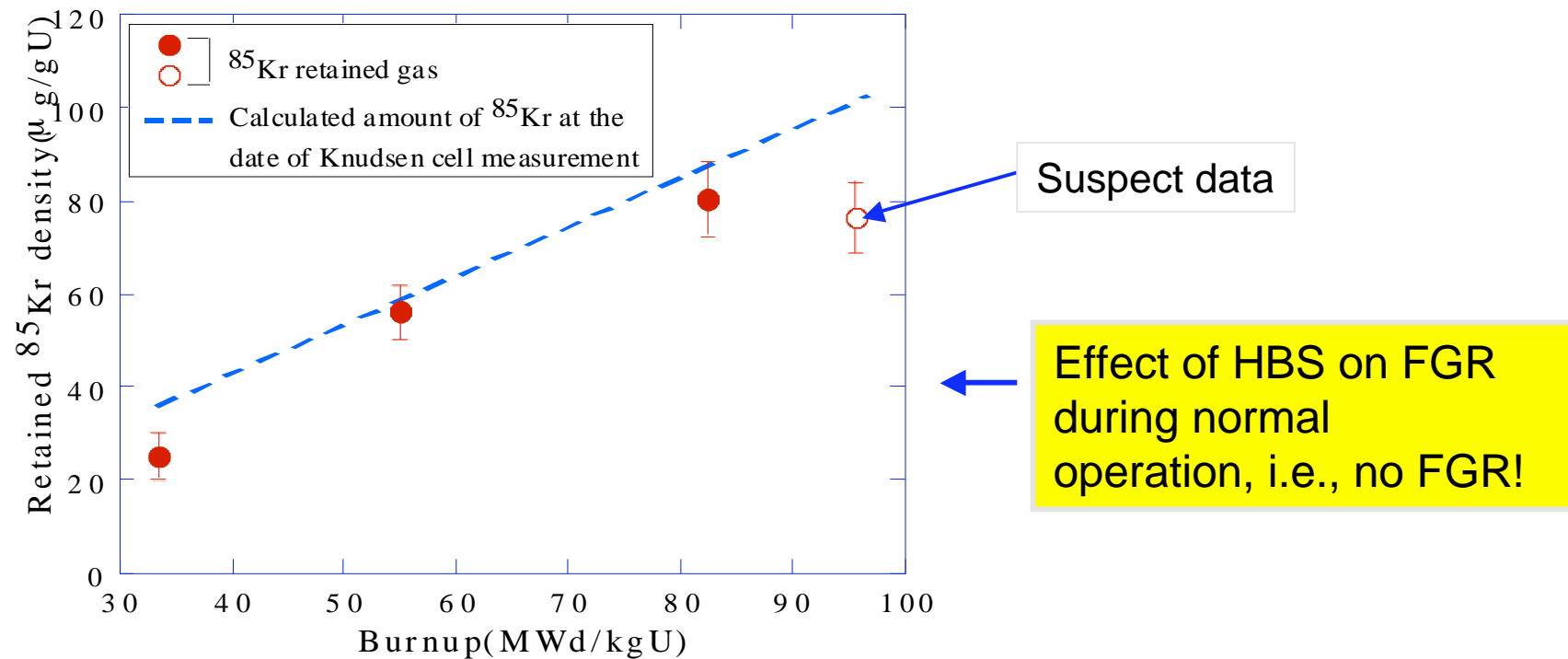




High burn-up Fuel

Some recent results from the HBRP

Kinoshita et al, ANS Orlando Florida September 2004





Resolution of grain boundary bubbles

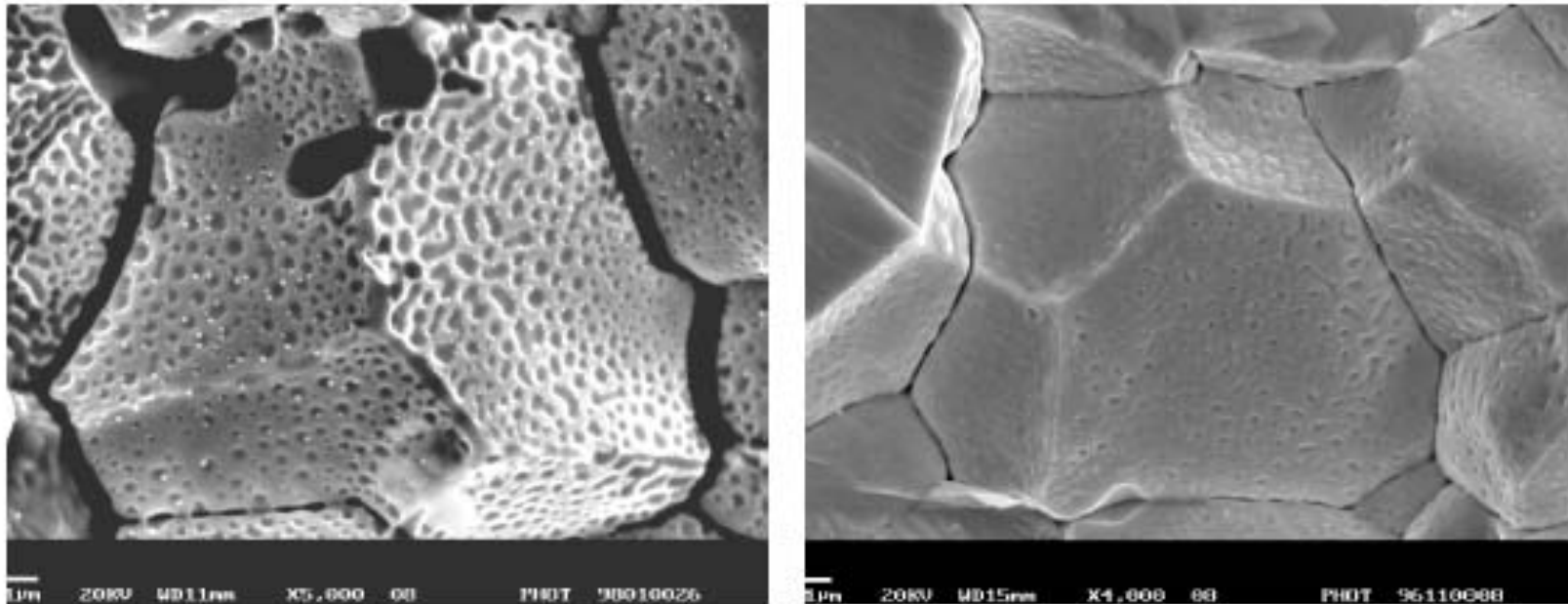


Figure 2: Grain-face images of fuel ramped in the 4162E and 4135E tests. The 4162E test (left) was discharged immediately after ramping while the fuel in 4135E (right) was held at low powers for an additional 28-days prior to discharge. Note the extensive denudation of the porosity in the extended-dwell test on the right.



Metallographic section, 38.8GWd/tU

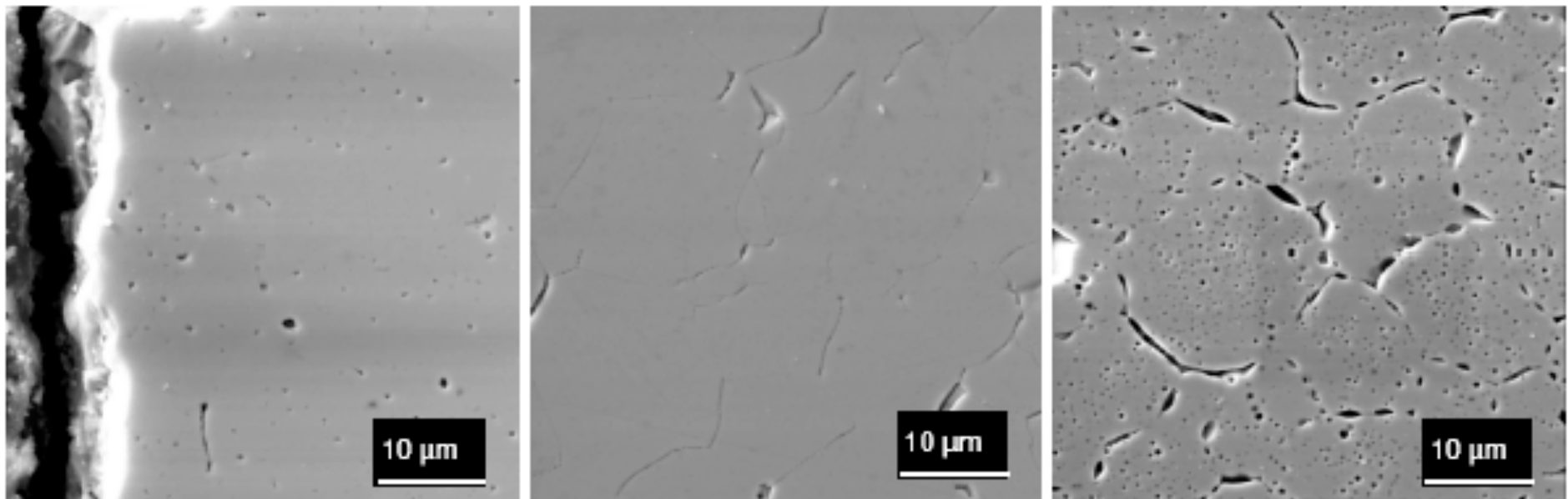


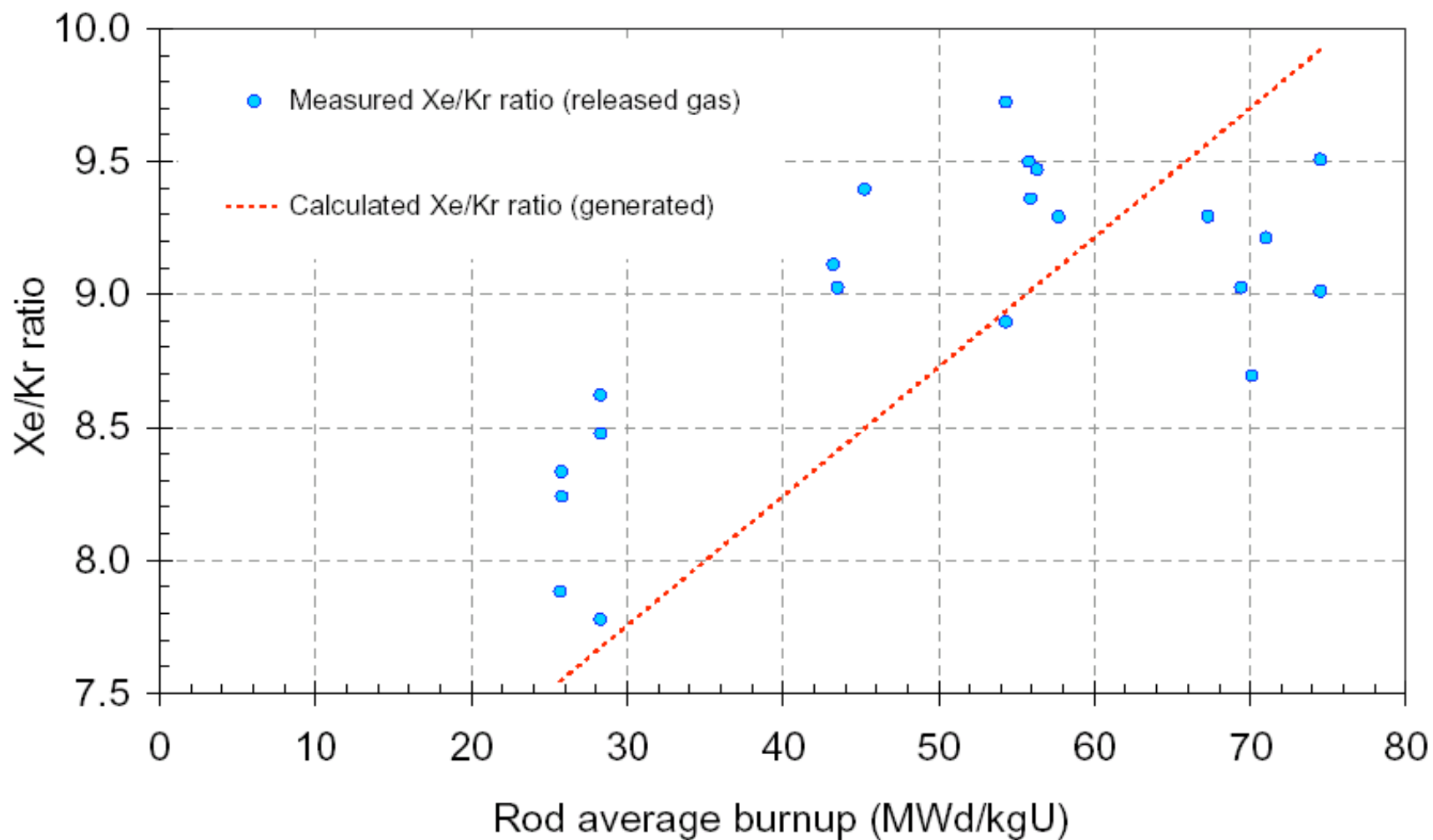
Figure 5 : SEM images of the fuel microstructure at the pellet edge (left photo), at mid-radius (centre photo) and in the pellet centre (right photo).



EXPERIMENTAL OBSERVATIONS ON FUEL PELLET PERFORMANCE AT HIGH BURNUP

J. Serna, P. Tolonen, S. Abeta, S. Watanabe, Y. Kosaka, T. Sendo, P. Gonzalez.
2005 Water Reactor Fuel Performance Meeting, Kyoto

Figure 5. Xe/Kr ratio vs. rod average burnup

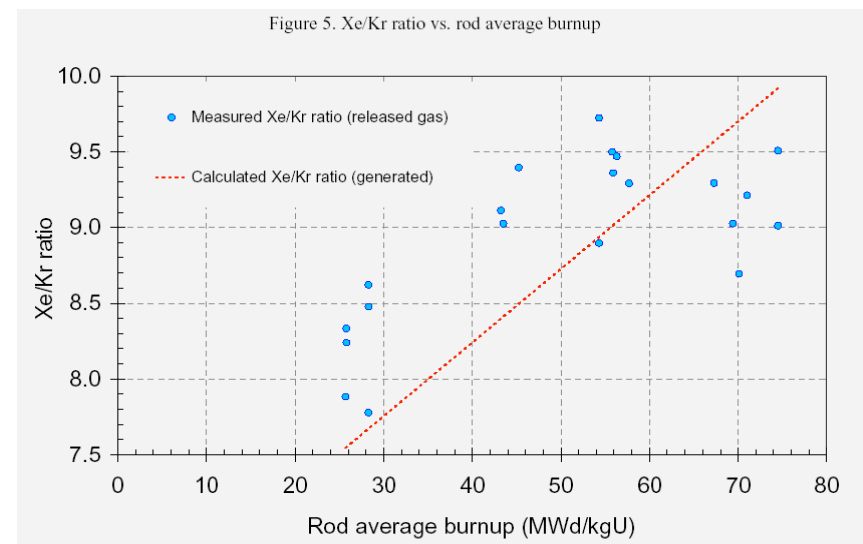




EXPERIMENTAL OBSERVATIONS ON FUEL PELLET PERFORMANCE AT HIGH BURNUP

J. Serna, P. Tolonen, S. Abeta, S. Watanabe, Y. Kosaka, T. Sendo, P. Gonzalez.
2005 Water Reactor Fuel Performance Meeting, Kyoto

Figure 5 shows the measured Xe to Kr ratio vs. burnup for the different pellet types after normal operation in Vandellós II. The dashed line in the figure presents the estimated generated ratio of these isotopes as a function of burnup. Taking into account the radial burnup distribution in the pellet, much higher in the pellet periphery than in the central part, and the different fission product yields as a function of burnup, this data can be used as a spatial (radial) indicator of the source of the released fission gases.

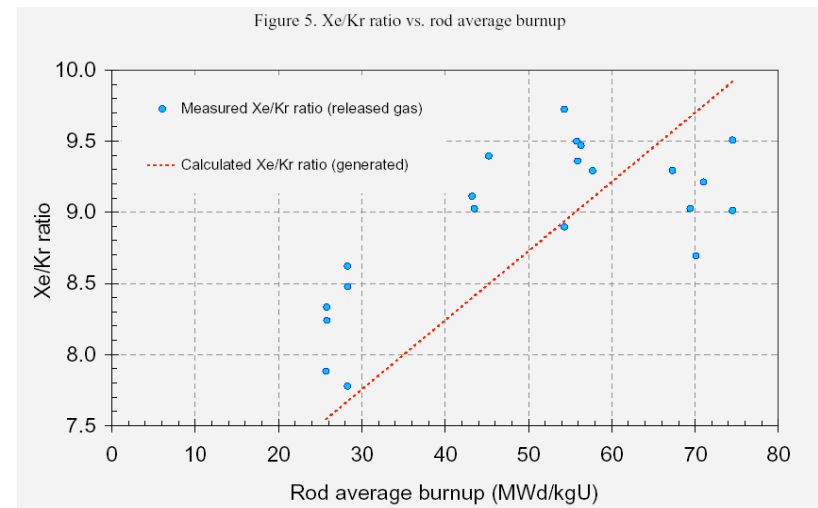




EXPERIMENTAL OBSERVATIONS ON FUEL PELLET PERFORMANCE AT HIGH BURNUP

J. Serna, P. Tolonen, S. Abeta, S. Watanabe, Y. Kosaka, T. Sendo, P. Gonzalez.
2005 Water Reactor Fuel Performance Meeting, Kyoto

Therefore, when the ratio Xe/Kr of the released gas is higher than that of the generated gas inventory at a given burnup, it can be interpreted that the gas release originates from a region with higher burnup than the pellet average. Despite that, in the highest burnup range, > 60 MWd/kgU, the high burnup structure is fully developed at pellet periphery, see Figure 9, the composition of the released gas suggest that no significant gas release has occurred at the pellet periphery. That is, the measured gas composition, coincides with that of gas generated locally at a burnup corresponding to the pellet centre, which is approximately 15-20% lower than the pellet average burnup. The data in Figure 5 reflects the opposite effect at lower burnup and also lower fraction of fission gas released. This observation is attributed to predominant athermal fission gas release from the pellet periphery.

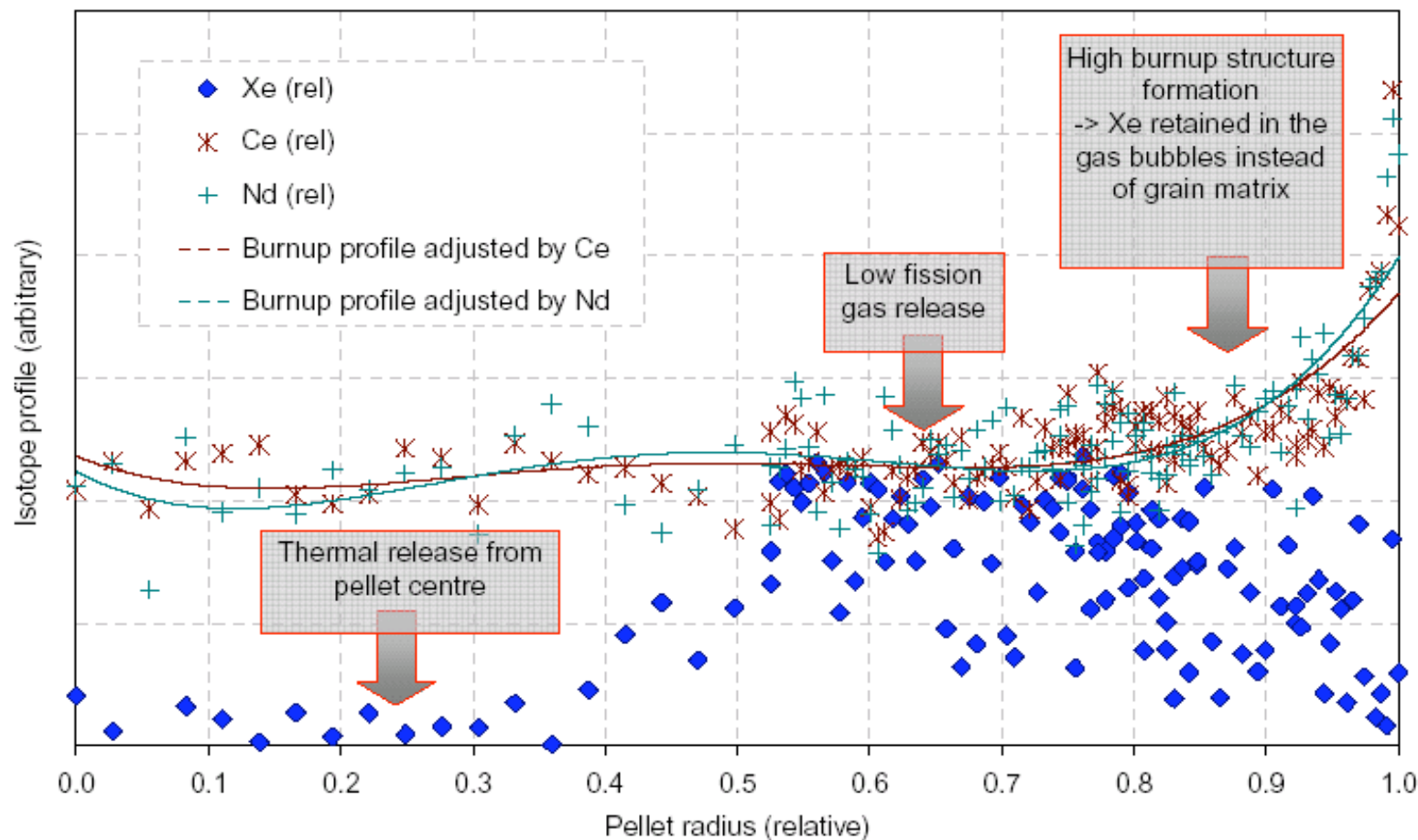




EXPERIMENTAL OBSERVATIONS ON FUEL PELLET PERFORMANCE AT HIGH BURNUP

J. Serna, P. Tolonen, S. Abeta, S. Watanabe, Y. Kosaka, T. Sendo, P. Gonzalez.
2005 Water Reactor Fuel Performance Meeting, Kyoto

Figure 6. EPMA data (burnup=81 MWd/kgU)





EXPERIMENTAL OBSERVATIONS ON FUEL PELLET PERFORMANCE AT HIGH BURNUP

J. Serna, P. Tolonen, S. Abeta, S. Watanabe, Y. Kosaka, T. Sendo, P. Gonzalez.
2005 Water Reactor Fuel Performance Meeting, Kyoto

Figure 8. Longitudinal ceramography (local burnup ~80 MWd/kgU)

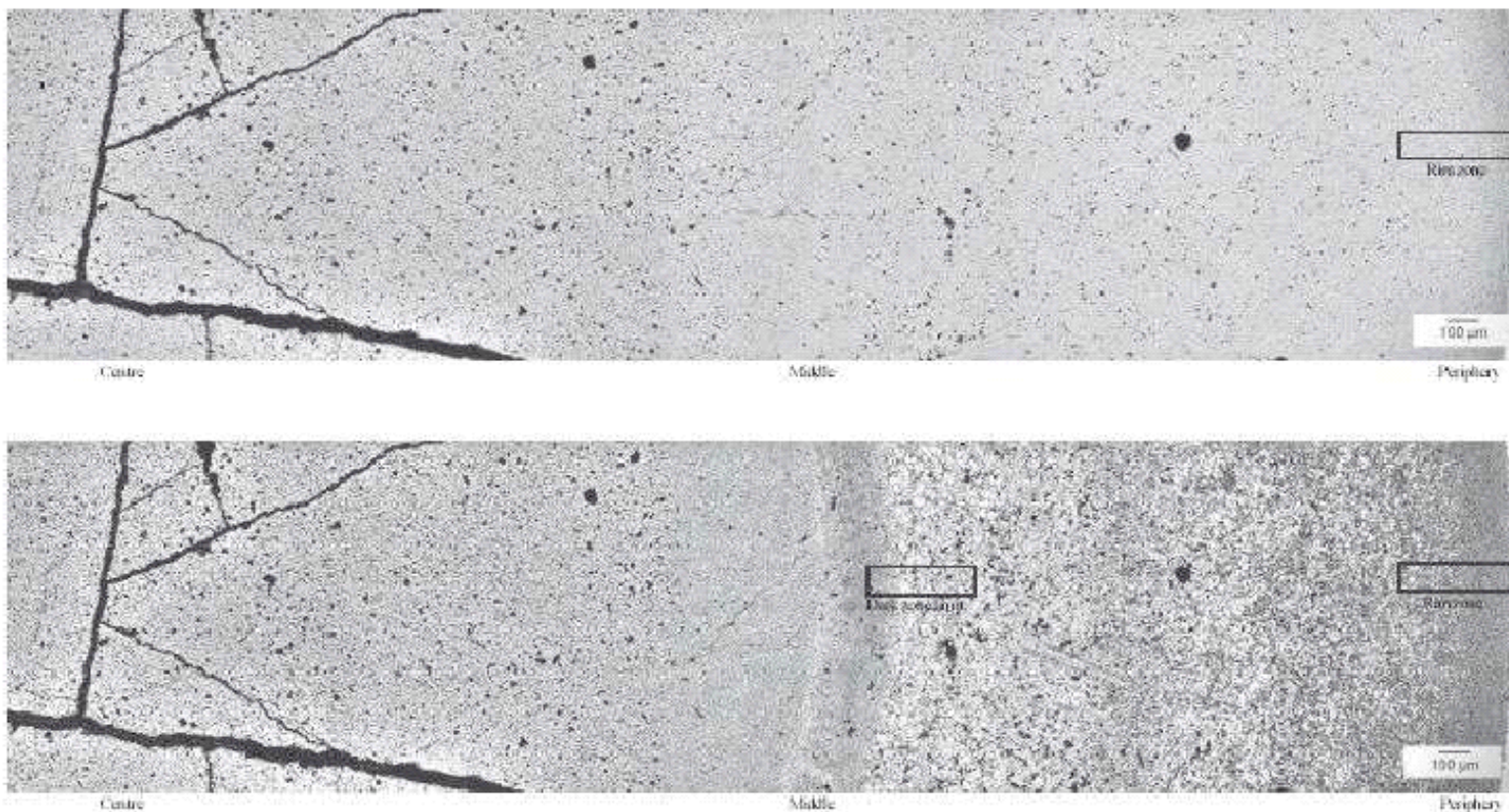




EXPERIMENTAL OBSERVATIONS ON FUEL PELLET PERFORMANCE AT HIGH BURNUP

J. Serna, P. Tolonen, S. Abeta, S. Watanabe, Y. Kosaka, T. Sendo, P. Gonzalez.
2005 Water Reactor Fuel Performance Meeting, Kyoto

Figure 9. Pellet ceramography. Radial overview (local burnup ~ 83 MWd/kgU).
Upper: polished fuel. Lower: Etched fuel.





Fuel Material behaviour

- Fuel swelling in power ramps
- Experimental results
 - Fission product distributions
 - Fission gas bubble resolution
- Swelling models
- Rim effects at high burnup



Industry goals

Looking for extended dwell of fuel

- Fission gas release
- Failure mechanisms
- Dimensional stability
- Frequent Fault (Class II) analysis
- Core design constraints
- Load follow



Industry goals

There are constraints on operation from PCI

- Conditioning of fuel
- Ramp rate restrictions
- Low power operation limits
- Frequent Fault (Class II) analysis
- Core design constraints
- Load follow



Impact for Fuel Modelling

- New fuel types, eg doped fuels
 - Diffusion coefficients
 - Creep
 - Limited data base
- New cladding materials
- Limited ramp testing



Impact for Fuel Modelling

➤ Rim effect modelling

- Swelling
- Fission gas release
- Interlinkage in the rim zone

➤ PCI modelling

- Mechanistic models
- Empirical rules
- New fuel types



Conclusions

The modelling shows good agreement for thermal behaviour and fission gas release at burnups close to current commercial limits (around 50MWd/kgU).

However, it is recognised that standard models do not account for an increase in fission gas release rates observed at high burnups and the teams have used various options and additional modelling in their codes to try to account for this phenomenon. Three distinct approaches have been tried:

1. Allowing fission gas release directly from the rim structure seen at the periphery of pellets at high burnup. Modelling choices include varying the retentive capacity of this region and in determining how to define the extent of the rim region. Evidence for this mechanism comes from the existence of the rim structure, which seems to initiate at the same time as the additional release. **However, there is much evidence that the rim does not release gas.**



Conclusions

The modelling shows good agreement for thermal behaviour and fission gas release at burnups close to current commercial limits (around 50MWd/kgU).

However,

2. Allowing release of additional gas from saturated regions of the fuel, where the saturation is temperature dependent and the additional release comes from the pellet interior. Modelling choices here lie in determining the saturation level and the temperature dependence of this effect. **However, there is no published experimental evidence for this effect.**
3. Allowing an additional burnup dependence on the diffusion parameters used in standard models. Release of fission gas is enhanced in the pellet centre with this approach. **This is a purely empirical approach with no theoretical justification.**



Conclusions

The modellers noted several important issues for high burnup modelling which will continue to be addressed during the remainder of the FUMEX-II CRP.

These include:

- Accurate calculations of the burn-up dependent radial power profile, i.e., Pu build-up at rim.
- What is the effect of the High Burnup Structure (HBS) at the rim? There is certainly a thermal barrier effect from the enhanced porosity.
- Is a separate treatment of this region required for successful modelling?
- What are appropriate conditions for the formation of the HBS?
- At what burnup does the enhanced release begin?
- What temperature limits should apply to the models?
- What are the effects of pressure, grain size, dopants or other details of fuel rod manufacture?

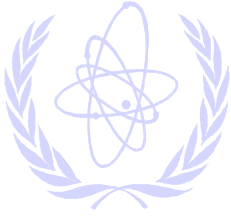


Conclusions

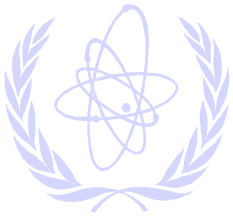
FUMEX-2

Additional priority cases have been determined for the participants to attempt during the final stages of the CRP. The data comes from the IFPE and considers experiments where the fuel reached burnups of around 60MWd/kgU –which is a little low – and where the PIE data includes fission gas release and fission product distributions in the pellets. They will use these to try to help to reach a consensus on some of these high burnup issues.

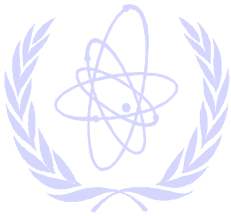
I'm afraid I cannot provide the answers today!



High Burnup Fuel pellet Rim									
CODE									
	Porosity limited	interlinkage small	FGR from rim	BU degradation of λ limited / reduced	Matrix swelling limited/reduced	Full porosity contribution to swelling	Temperature limit for Rim formation	Influence of stress and/or grain size on rim formation	Separate treatment of transition zone
1	-	no	no	-	-	-	no	-	-
2	no extra rim porosity	-	no	-		no	no		
3	-	-	no	-		-	-		
4	no limit	no interlinkage modelled	no	no	no	yes	no limit	no	no
5	yes	no	yes?	yes		no	yes		
6	yes	yes	yes	yes	yes	yes	yes	no, mere dependence on local BU	no
7	no	no	no	yes		yes	-		
8	no	no	yes	yes	no?	no?	no	no	no
9	no	no	yes	yes	no	no	yes	no	no
10	no limit	yes	no	no (mechanistic model)	no	yes	no limit but depending on Temp	no	no
11	no limit	not applicable	no	mechanistic concept		yes	no limit		yes
12	No	Yes	yes	Yes		No	Yes	No	No
13	no limit	no	no	no/no		no	no/yes		
14	limit	no	yes	no	no	yes	no	no	no
15	no limit	-	yes	no	no	yes	no	no	no
16	no limit	not always	yes	no, hardly ever goes to zero	yes, in line with Xe depletion	yes	yes, T-dependent functional	yes&yes	no, model applicable throughout
17	15% limit	-	yes, saturation	no		yes	no limit		
18	15% limit	no	yes, saturation	no		yes	no limit		
19	15% limit	-	yes, saturation	no		yes	no limit		



CODE	High BU Fission Gas Release								
	Diffusion coefficients for FGR			Xe concentration limit			Main contribution to high BU FGR		
	BU enhancement of thermal diffusion coefficient	BU enhancement of athermal diffusion coefficient	"Phase transition" of diffusion coefficients	Rim	Transition zone	thermal interior zone	from rim	from transition zone	from pellet interior
1	no	no	-	no	yes	yes	-	-	yes
2	yes	yes		-	no	no			
3	no	yes		no	no	no			
4	no	no	no	no	N/A	no	zero	zero	1
5	no	no		no	no	no			
6	no	no	no	yes	yes	yes	no	yes	yes
7	no	no		-					
8	no	no	no	no	?	?	no	yes	yes
9	no	no	no	yes	yes	yes	no	no	yes
10	no	no	no	yes	no	no			yes
11	mechanistic yes	no		yes-mechanistic	yes-mechanistic	yes-mechanistic			
12	Yes	no	no	no	no	no			
13	no/yes?	no		no	no	no			
14	no	no	no	yes	no	no			
15	no	no	no	no	no	no	yes	no	yes
16	no	no	no	no	no	no	yes, possible	no, hardly ever	yes, possible
17	no	no		yes	no	no			
18	no	no		-	no	no			
19	no	no		yes	no	no			



CODE	Re-solution				Radial Power	Other mechanisms	Local BU for start of rim restructuring
	intragranular	intergranular	inter/intra dep. on BU	inter/intra dep. on Temperature			
1	not applicable	not applicable	not applicable	not applicable	no	Empirical model	no RIM
2							-
3							-
4	irradiation induced only	irradiation induced only	no/no	no/yes	yes	no	40 MWd/kgU pellet average
5							45 pellet av
6	yes	yes	no	yes	yes		68 MWd/kg
7							calculated ca. 60
8	yes	yes		yes			48.8
9	yes	yes	yes	yes	yes	Bonding	yes 48.8
10							not BU dependent (mechanistic model)
11							calculated 45-60
12	Yes	Yes	Yes	Yes	Yes		
13							yes ?
14	yes					Microcracking	55
15	no	yes	no	yes	no		28.8 pellet av
16	yes	no	no, intra/mechanistic	no, intra/mechanistic	Yes	Yes, there are	no, another concept
17							60
18							60
19							60

